ACS OMEGA

Open Access

http://pubs.acs.org/journal/acsodf

Article

Artesunate Alleviates Kidney Fibrosis in Type 1 Diabetes with Periodontitis Rats via Promoting Autophagy and Suppression of Inflammation

Chen Liang,[‖] Licheng Ma,[‖] Yi Chen, Jiaquan Li, Binge Wang, Chubin Ma, Zhong Yuan, and Xiaolin Nong*

Cite This: *ACS Omega* 2024, 9, 16358−16373

Read Online

ACCESS | Metrics & More | Article Recommendations

ABSTRACT: To explore the effect of periodontal disease on the progression of diabetic kidney disease (DKD), to observe the effects of artesunate (ART) intervention on periodontal and kidney tissues in type 1 diabetic rats with periodontitis, and to explore the possibility of ART for the treatment of DKD. Rat models of diabetes mellitus, periodontitis, and diabetes mellitus with periodontitis were established through streptozotocin (STZ) intraperitoneal injection, maxillary first molar ligation, and P. gingivalis ligation applied sequentially. Ten weeks after modeling, ART gavage treatment was given for 4 weeks. Immunohistochemistry, reverse transcription-quantitative polymerase chain reaction (RT-qPCR), and Western blot were used to investigate the inflammatory factors, fibrogenisis, autophagy-related factors, and proteins in periodontal and kidney tissues, and 16S rDNA sequencing was used to detect the changes in dental plaque fluid and kidney tissue flora. Compared to the control group, the protein expression levels of transforming growth factor β1 (TGF-β1) and COL-IV in the periodontal disease (PD) group were increased. The protein expression of TGF-β1, Smad3, and COL-IV increased in the DM group and the DM + PD group, and the expression of TGF-β1, Smad3, and COL-IV was upregulated in the DM + PD group. These results suggest that periodontal disease enhances renal fibrosis and that this process is related to the TGF-β1/Smad/COL-IV signaling pathway. Among the top five dominant bacteria in the kidney of the DM + PD group, the abundance of *Proteobacteria* increased most significantly, followed by Actinobacteria and Firmicutes with mild increases. The relative abundance of Proteobacteria, Actinobacteria, and Firmicutes in the kidney tissues of DM and PD groups also showed an increasing trend compared with the CON group. Proteobacteria and Firmicutes in the kidney of the PD group and DM + PD group showed an increasing trend, which may mediate the increase of oxidative stress in the kidney and promote the occurrence and development of DN. Periodontal disease may lead to an imbalance of renal flora, aggravate renal damage in T1DM, cause glomerular inflammation and renal tubulointerstitial fibrosis, and reduce the level of autophagy. ART delays the process of renal fibrosis by inhibiting the TGF-β-Smad signaling pathway.

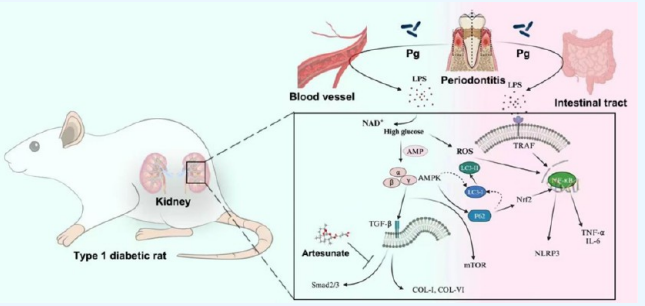

1. INTRODUCTION

As one of the most common and serious microvascular lesions in diabetes mellitus, diabetic kidney disease (DKD) is characterized by persistent proteinuria and the progressive deterioration of renal function. The pathological changes are characterized by diffuse glomerular basement membrane thickening, mesangial matrix hyperplasia, Kimmelstiel−Wilson nodule formation, and tubulointerstitial fibrosis, resulting in glomerulus sclerosis and renal tubule wasting.[1] The pathogenesis of DKD is not fully understood, and it is believed to be closely related to renal injury mediated by autophagy disorder, oxidative stress, inflammatory response, and other factors under high glucose conditions.[1,2] Therefore, through the establishment of the diabetic rat model, we expect to explore autophagy dysfunction and inflammation in the DKD concrete mechanism.

Periodontal disease (PD) is a chronic infectious disease originated in the gingiva and is caused by bacteria in dental plaque, and it is characterized by tooth loss and irreversible alveolar bone loss.[3] In recent years, studies have shown that periodontal disease contributes to the development of various

Received: January 2, 2024
Revised: February 21, 2024
Accepted: February 26, 2024
Published: March 29, 2024

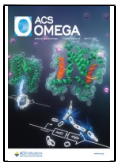

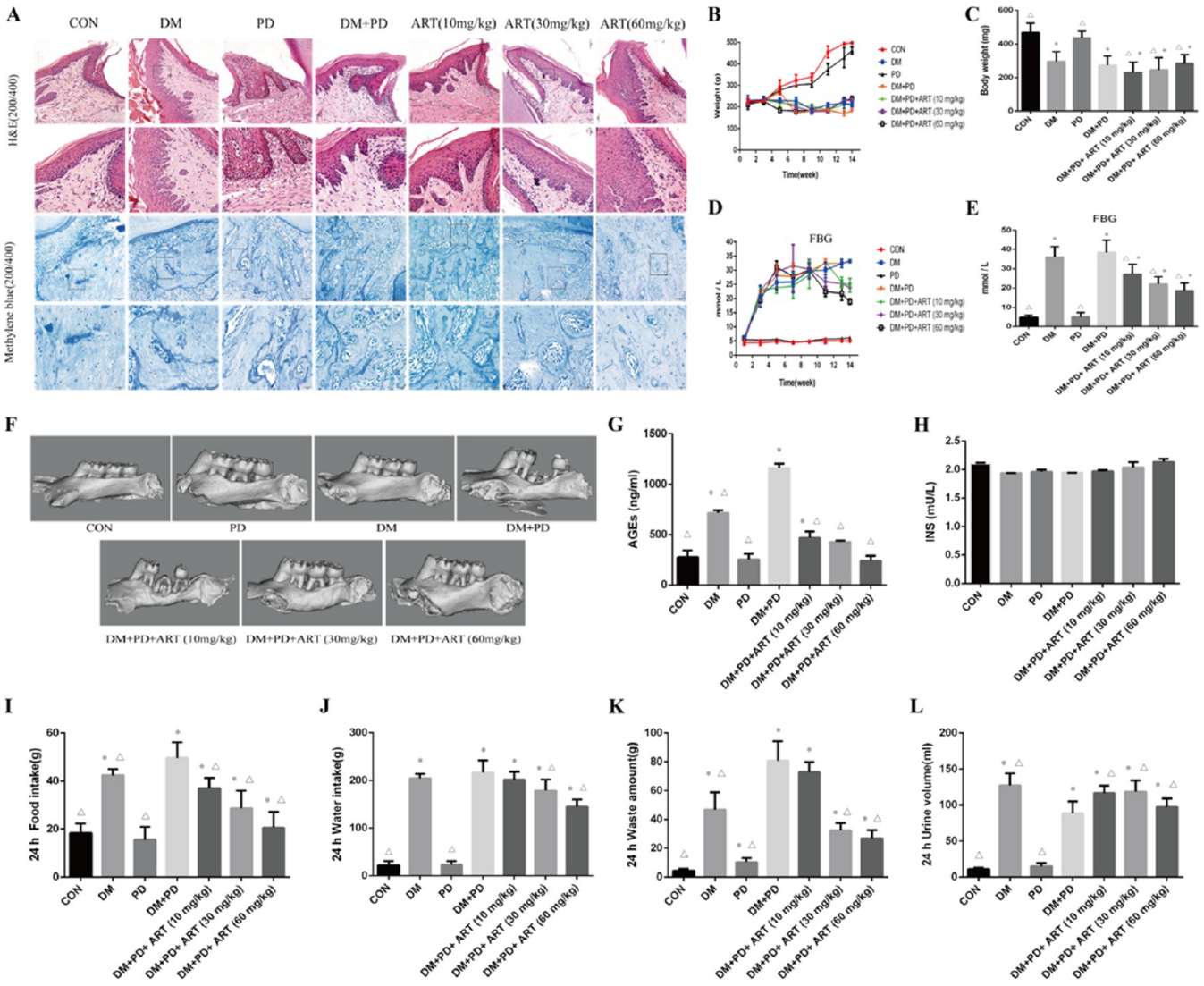

Figure 1. Establishment of a rat model of diabetic periodontitis and detection of metabolic indexes. (A) HE and methylene blue staining of periodontal tissue. (B, C) Dynamic measurement of rats body weight. (D, E) model blood glucose dynamic measurement indicators. (F) Three-dimensional (3D) reconstructed micro-CT images of rat periodontal tissues. (G−L) 24H blood metabolic parameters of rats. $^{*}P < 0.05$, the results of each group were compared with the CON group. $^{\Delta}P < 0.05$, the results of each group were compared with the DM + PD group.

systemic diseases as a chronic inflammatory response beyond just affecting periodontal tissue. These diseases include diabetes mellitus, cardiovascular disease, kidney disease, etc. In 2005, it was first confirmed that periodontal disease is related to renal insufficiency, and the incidence of decreased glomerular filtration rate in patients with periodontal disease is twice of that in patients without periodontal disease,[4,5] suggesting that periodontal disease may aggravate the occurrence of chronic kidney disease (CKD). Its mechanism may have a positive correlation with the occurrence of bacteremia mediated by periodontal inflammatory factors and the damage of renal endothelial cells. Sawa et al. found that lipopolysaccharide (LPS) increases the accumulation of type I collagen in glomeruli, causes glomerulosclerosis, and mediates the production of urinary protein. These findings support that periodontal disease aggravates the progression of DKD.[6] Fang et al. reported that periodontal treatment improves renal inflammatory response and reduces the incidence of CKD.[7] Periodontal treatment may reverse the development of kidney disease by reducing the release of local inflammatory factors, regulating the glomerular filtration rate, and decreasing serum creatinine.[8]

The AMPK/mTOR pathway is one of the main pathways regulating autophagy, where AMPK indirectly regulates autophagy through mTOR.[9] AMPK regulates mTOR both directly and indirectly. On one hand, when intracellular energy is reduced, AMPK, a sensitive energy signal sensor, is activated through the phosphorylation reaction, resulting in inhibition of mTOR. Decreased activity of mTOR leads to an enhanced autophagy process.[10] On the other hand, phosphorylated AMPK inhibits mTOR activity and indirectly enhances autophagy by phosphorylating the TSC1/2 complex.[10] Podocyte injury is the hallmark event of glomerular disease in the early stage of DKD.[1] The activation of the mTOR signaling pathway promotes podocyte hypertrophy to adapt to the glomerular hyperfiltration state, but compensatory hypertrophy can accelerate podocyte loss, thereby forming a vicious cycle of podocyte hypertrophy and loss.[11,12] At the same time, the decreased autophagic flux of podocytes also causes progressive loss of renal function.[1] In the middle and late

https://doi.org/10.1021/acsomega.4c00020
ACS Omega 2024, 9, 16358−16373

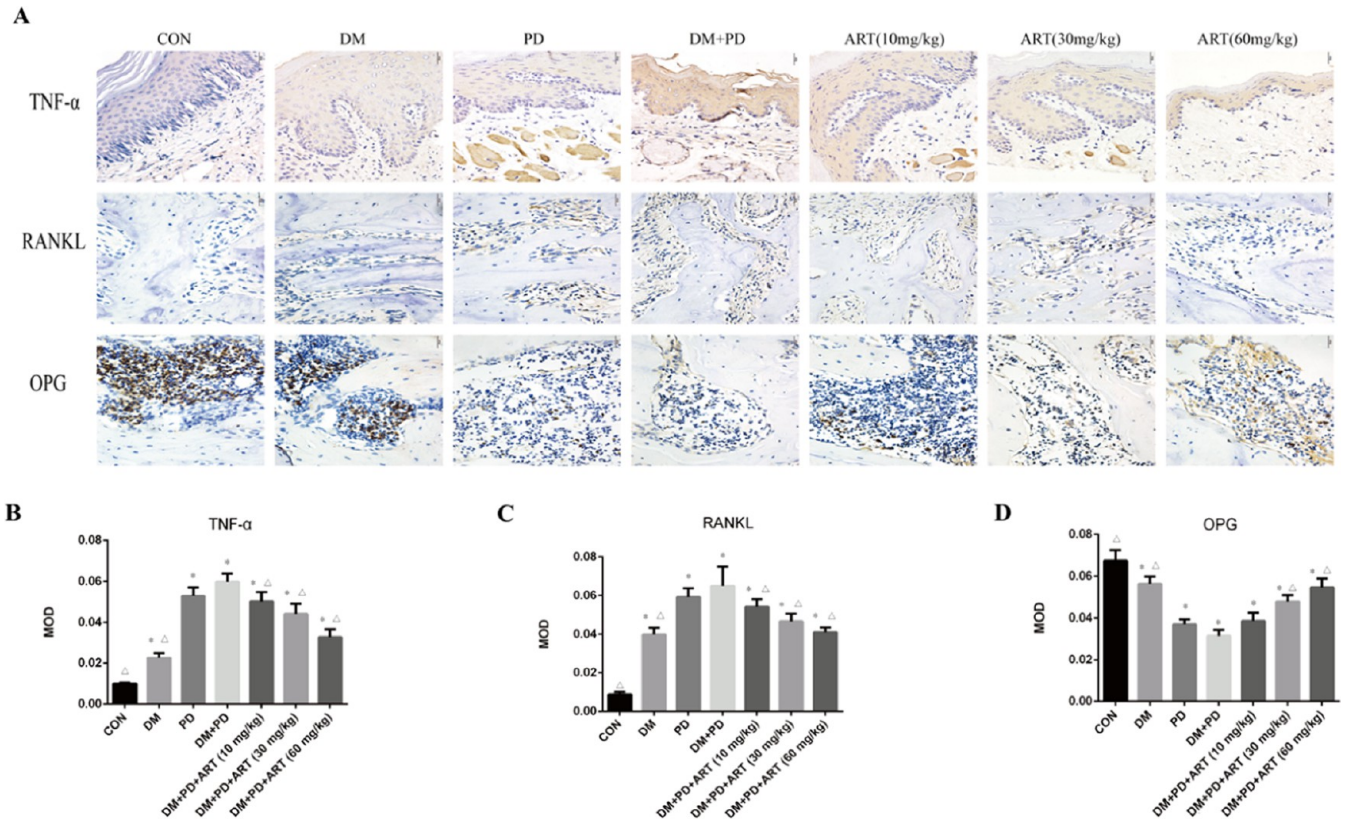

Figure 2. Periodontal inflammation index of the model was detected. (A) IHC of the three indicators. (B−D) Quantitative analysis of the IHC results.*$P < 0.05$, the results of each group were compared with the CON group. $^{\Delta}P < 0.05$, the results of each group were compared with the DM + PD group.

stages of DKD, the excessive proliferation, apoptosis, and extracellular matrix (ECM) accumulation of glomerular mesangial cells directly aggravate the degree of proteinuria and glomerulosclerosis. Inhibition of the mTOR signaling pathway reduces oxidative stress and increases autophagy levels, thereby preventing the above pathological process.[13]

The accumulation of the glomerular extracellular matrix (ECM) is the pathological basis of glomerulosclerosis.[12,14] Plasminogen and plasminogen activator inhibitor-1 (PAI-1), the key factors in the fibrinolytic system, play an important role in ECM degradation, and their abnormal expression leads to ECM accumulation, glomerulosclerosis, and renal tubulointerstitial fibrosis.[12,15] Transforming growth factor β1 (TGF-β1) is an important fibrogenic factor. High expression of TGF-β1 increases the production of ECM in mesangial cells and stimulates the increase of type IV collagen (COL-IV), the main component of ECM, thereby promoting renal interstitial fibrosis.[16,17] The imbalance of the fibrinolysis system and the high expression of TGF-β1 causes internal environment disorder and activates a variety of signaling pathways in the kidney; as a result, it promotes the process of fibrosis and aggravates the deterioration of renal function. The autophagy activity of renal intrinsic cells such as podocytes and mesangial cells is decreased in diabetic nephropathy model mice,[18] which weakens the ability of renal intrinsic cells to remove damaged proteins and organelles in time, resulting in renal intrinsic cell damage, which leads to thickening of glomerular basement membrane and increase of ECM, and promotes renal fibrosis.[19] Therefore, increasing the level of autophagy in renal tissue and inhibiting the high expression of TGF-β may be effective targets for delaying the progression of renal fibrosis.

Artemisinin is a sesquiterpene lactone with a peroxide group extracted from Artemisia (a natural plant used as traditional medicine in China).[20] Artesunate (ART, $C_{19}H_{28}O_8$, molecular weight 384.42), a derivative of artemisinin, has been widely used in clinical practice orally and intravenously as a safe and effective antimalarial drug.[21] Previous studies from our lab have revealed that ART plays important roles in immune status,[22] anti-inflammation response, blood glucose,[23] and inhibition of bone resorption.[24] However, whether ART regulates the occurrence and development of DKD by regulating the level of autophagy remains unknown. We established a rat model of diabetes with periodontitis to explore whether periodontitis could affect the progression of DKD through the dysbiosis of microbiota. At the same time, we performed ART intervention in rats to explore whether the anti-inflammatory and antibacterial effects of ART are effective for DKD and the specific mechanism behind the action of ART.

2. MATERIALS AND METHODS

2.1. Animals. All animal procedures were approved by the Institutional Animal Ethics and Committee of The Guangxi Medical University (ethics number: 201808310). Male, weight about 250 ± 20 g, Sprague-Dawley rats were used in this study and housed in a specific-pathogen-free level laboratory for at least 1 week before experiments. Each group of rats was kept in a 12 h alternating light/dark cycle at 25 ± 2 °C and 60% humidity. The rats were randomly divided into the treatment

https://doi.org/10.1021/acsomega.4c00020
ACS Omega 2024, 9, 16358−16373

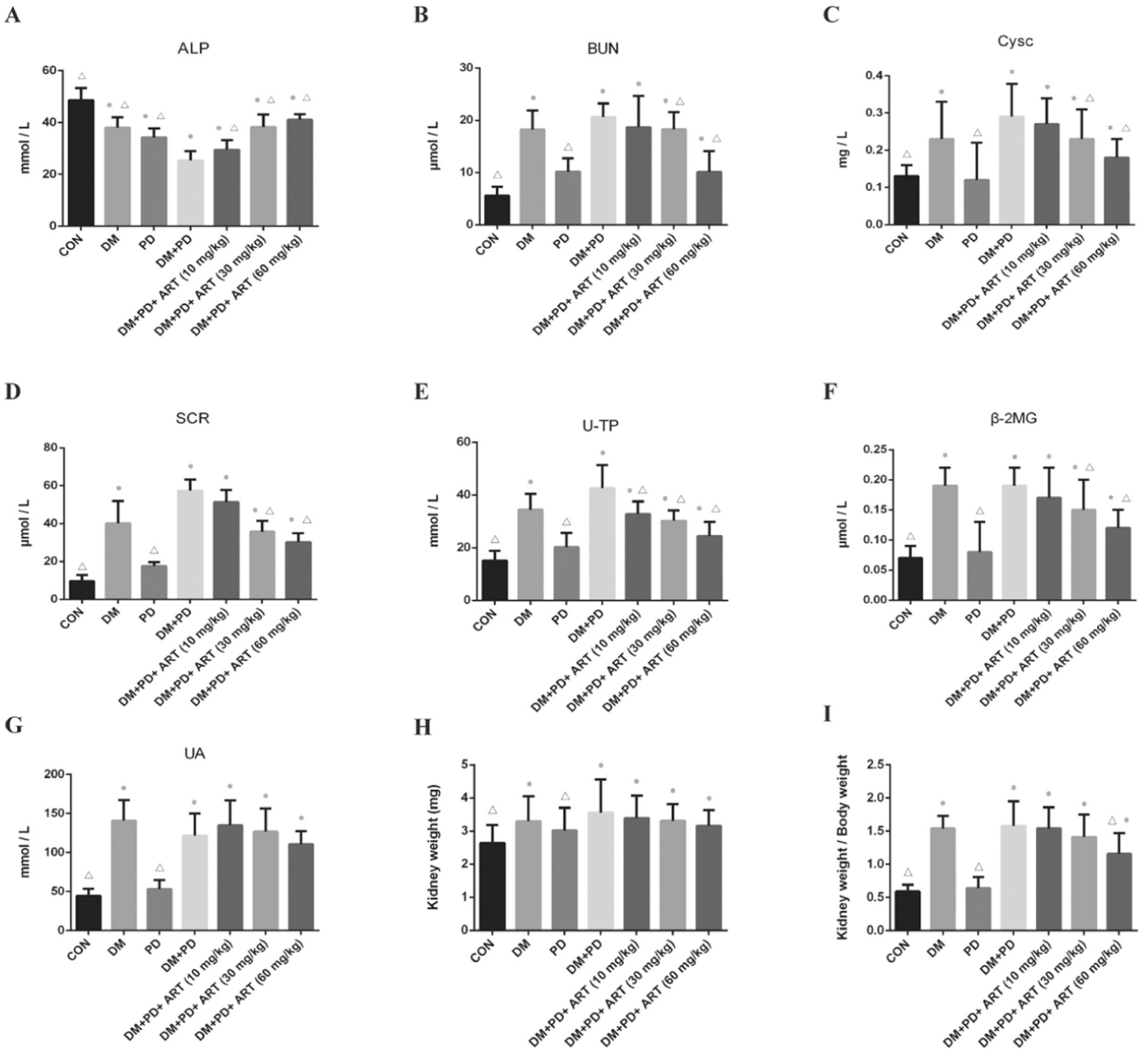

Figure 3. Renal function indexes (A: ALP, B: BUN, C: Cysc, D: Scr, E: U-TP, F: β2-MG, G: UA), kidney weight (H), and KI (I) were analyzed at the end of the experiment. $^{*}P < 0.05$, the results of each group were compared with the CON group. $^{\Delta}P < 0.05$, the results of each group were compared with the DM + PD group.

group and the control group (CON) with 8 mice in each group.

2.2. Diabetic Periodontal Disease Animal Grouping. Seven groups include the control group (CON), the periodontal disease group (PD), the type I diabetes mellitus group (DM), the type I diabetic periodontal disease model group (DM + PD), the 10 mg/kg artesunate treatment group [DM + PD + ART (10 mg/kg)], the 30 mg/kg artesunate treatment group [DM + PD + ART (30 mg/kg)], and the 60 mg/kg artesunate treatment group [DM + PD + ART (60 mg/kg)] (n = 8). First, rats in the DM group were injected intraperitoneally with STZ (60 mg/kg), and the CON group and PD group were administrated intraperitoneally with the same amount of PBS. After 72 h, rats were measured for blood glucose at ≥16 7 mmol/L, eliminating noncompliant rats. One week later, an 8-0 silk ligature was tied around the right maxillary first molars in rats after injecting the P. gingivalis (0.1 mL) into the gums once daily from the second week to the fifth week to establish the rats model of the PD model. Rats' blood glucose was measured weekly. The doses of ART of 10, 30, and 60 mg/kg/d were administered intragastrically on the fifth week after model establishment, while the other 4 groups received PBS solution.

2.3. Periodontitis and Diabetes Assessment. Periodontal bleeding index and tooth looseness were assessed every 2 days to determine the severity of periodontitis. Blood sugar levels, body weight, food intake, stool volume, and urine volume were measured in each group at the start of treatment and once weekly for 4 weeks afterward. Serum levels of INS and AGEs were detected by ELISA.

2.4. Periodontal Tissue Collection and Sample Preparation. In the fourth week after successful modeling

https://doi.org/10.1021/acsomega.4c00020
ACS Omega 2024, 9, 16358−16373

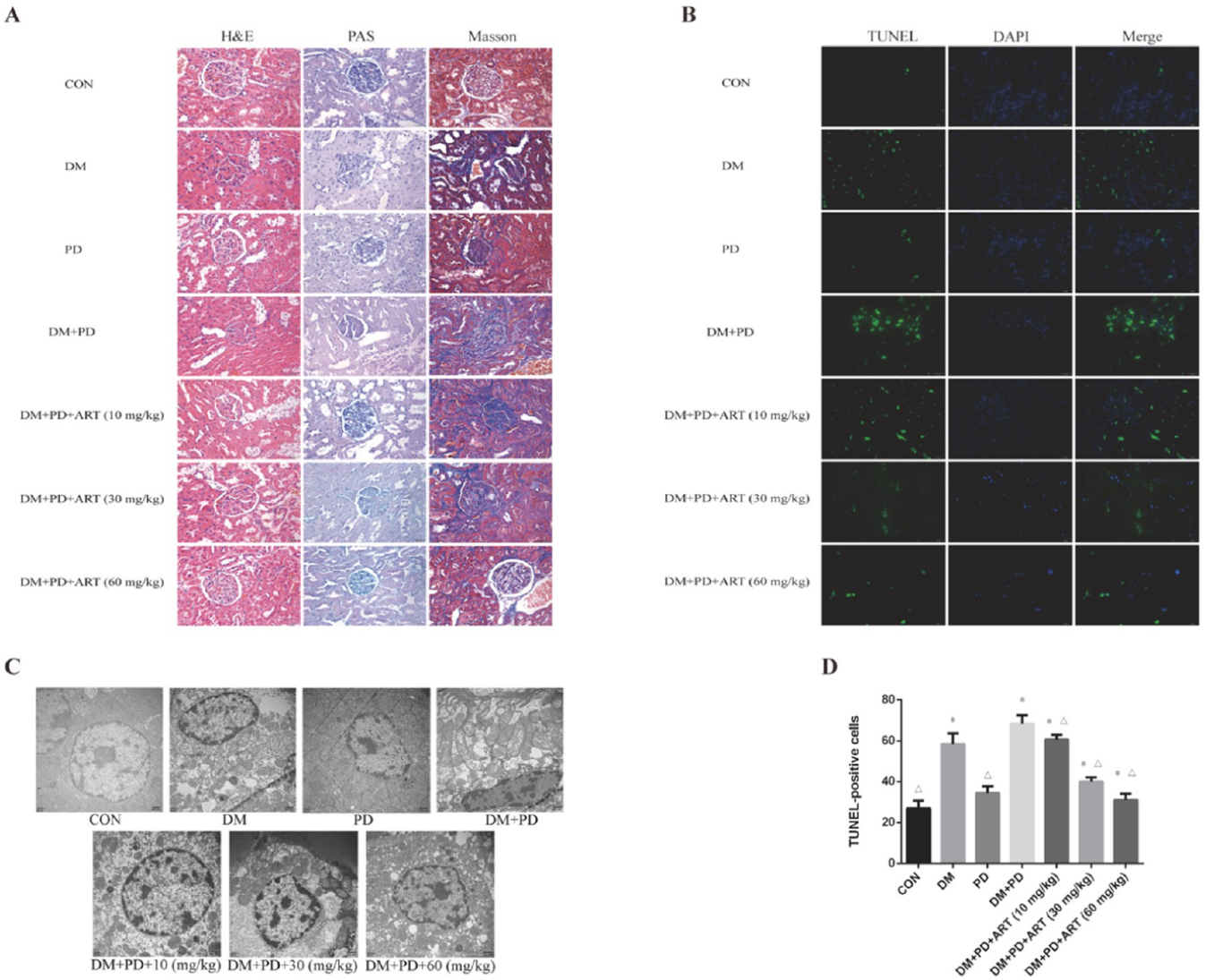

Figure 4. Periodontitis aggravates diabetic nephropathy. (A) H&E, PAS, and Masson staining of the kidney tissue. (B) TUNEL expression in the kidney tissue of rats in each group. (C) Transmission electron microscopy (TEM) image observation of kidney tissue. (D) Gray-scale bar graph of TUNEL. $^{*}P < 0.05$, the results of each group were compared with the CON group. $^{\Delta}P < 0.05$, the results of each group were compared with the DM + PD group.

of periodontal disease, the maxillary alveolar bone of the rats was collected and fixed for 24 h (4 °C formalin). Micro-CT scanning was performed to analyze the bone resorption of one side of the alveolar bone (Toyo Corporation, Tokyo, Japan). Data Viewer image editing software (Bruker, Kontich, Belgium) performed the necessary corrections. The other side of the maxillary alveolar bone was decalcified with 10% ethylenediaminetetraacetic acid (EDTA) for 8 weeks, embedded in paraffin, and cut into 4 μm serial sections for hematoxylin and eosin (H&E) staining, methylene blue staining, and immunohistochemical analysis.

2.5. Measurement of Serological Parameters and Kidney Function. After 4 weeks of ART intervention, rats were sacrificed, and samples were collected. Kidney function can be measured by the parameter percent organ mass (organ mass/body weight * 100). Blood samples were obtained by cardiac puncture and promptly transported to the Affiliated Tumor Hospital of Guangxi Medical University (Guangxi, China) for determination of serum terminal blood glucose, serum creatinine, urea nitrogen, endogenous creatinine clearance, and 24 h urinary albumin levels.

2.6. Mitochondrial Morphology Observation by Electron Microscopy. The fresh renal cortex (about 1 mm^3 in area) was collected, fixed, embedded, sectioned, and stained according to the operating procedures of a transmission electron microscope (TEM). Finally, the renal tubular epithelial cells were observed, and the images were collected.

2.7. Measurement of Kidney Cell Apoptosis. Apoptotic activity was evaluated by detecting the level of apoptosis in kidney sections made in Section 2.6 using a kit (Beijing Bioss Biotechnology Co., Ltd., Beijing). The number of apoptotic cells in kidney tissue was observed under a microscope (X40), and the apoptotic index (number of apoptotic cells in visual field/total number of cells in visual field × 100) was calculated.

2.8. Computer Molecular Docking Was Used to Simulate the Detailed Binding Mode of ART with AMPK, mTOR, and TGF-β1. To investigate how artesunate interacts with TGF-β, AMPK, and mTOR, computational simulations were performed. The optimal docking posture with

https://doi.org/10.1021/acsomega.4c00020
ACS Omega 2024, 9, 16358−16373

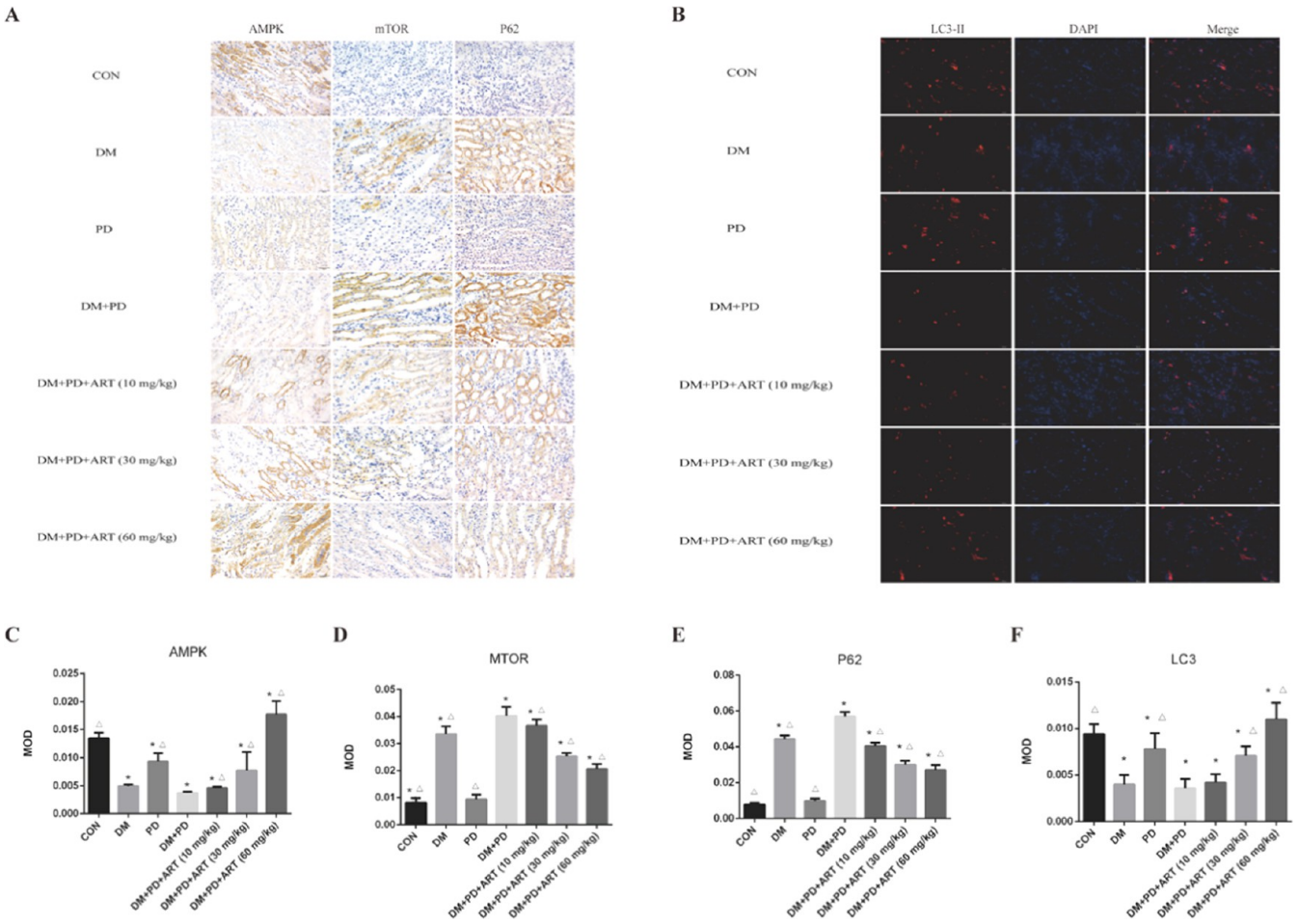

Figure 5. Type 1 diabetes with periodontitis induced renal injury via autophagy. (A) Immunohistochemical staining of AMPK, mTOR, and P62 for the kidney tissue (200×). (B) Immunohistochemical staining of LC3-II for the kidney tissue. (C−F) Gray-scale bar graph of immunohistochemistry. $^{*}P < 0.05$, the results of each group were compared with the CON group. $^{\Delta}P < 0.05$, the results of each group were compared with the DM + PD group.

the lowest energy for the interaction of artesunate with the above targets is presented to further investigate the detailed binding mode of artesunate; the interaction was analyzed by residue-by-residue free energy. The molecular docking simulation between artesunate and each protein showed that the docking binding energy between artesunate and each protein was less than 0 in the initial screening results, indicating that artesunate and each protein could bind naturally. Among them, artesunate forms hydrophobic interaction with amino acid residues LEU-364, PRO-314, and ARG-85 on the active site of the TGF-β chain. These forces enable artesunate to firmly bind to the active site of TGF-β. In addition, as shown in the figure, artesunate is closely bound to amino acid residues in the active sites of AMPK and mTOR chains by hydrophobic interaction, indicating that this study has research value.

2.9. Hematoxylin−Eosin, Methylene Blue Staining, PAS, Masson Staining, Immunohistochemistry, and Immunofluorescence Staining. To examine the periodontal histological features, we performed HE, methylene blue staining, and immunohistochemical staining (TNF-α, RANKL, and OPG). To examine renal histological features, we performed PAS, Masson staining, and immunohistochemical staining for NF-κB, TNF-α, TGF-β, Smad2, COL-VI, AMPK, mTOR, and P62. LC3-II was detected by immunofluorescence staining (1:800 dilution; Cell Signaling Technology, Boston, MA)

2.10. Reverse Transcription-Quantitative Polymerase Chain Reaction (RT-qPCR). RT-qPCR was performed using the method in a previous study. After data collection, the $\Delta\Delta$Ct method was used to calculate the relative expression of each mRNA after normalization to β-actin. Information on all primers is listed in Table 1.

2.11. Western Blot. By centrifuging samples at 12,000*g* for 8 min at 4 °C, protein was collected from kidneys, and quantification was performed using the Bradford method Bio-Rad Protein Assay (Hercules, CA) following the manufacturer's instructions. Sodium dodecyl sulfate-polyacrylamide gel electrophoresis (SDS-PAGE) was then performed on protein extracts (50 mg protein/sample), and poly(vinylidene fluoride) (PVDF) membranes were applied (Millipore). Primary antibodies were applied to the blots (1:1000) except for anti-AMPK (1:2000), anti-LC3-II (1:500), and anti-TGF-β (1:500), followed by secondary antibodies (1:5000). To detect specific proteins, ECL chemiluminescent substrate (Millipore, MA) was used according to the manufacturer's instructions. Quantification was done with Image Quant version 5.1.

2.12. 16S Sequencing Analysis of Rat Oral Swabs and Kidney Tissue. 16S sequencing analysis was performed on DNA from rat oral swabs and renal aortic arch tissue, and PCR

https://doi.org/10.1021/acsomega.4c00020
ACS Omega 2024, 9, 16358−16373

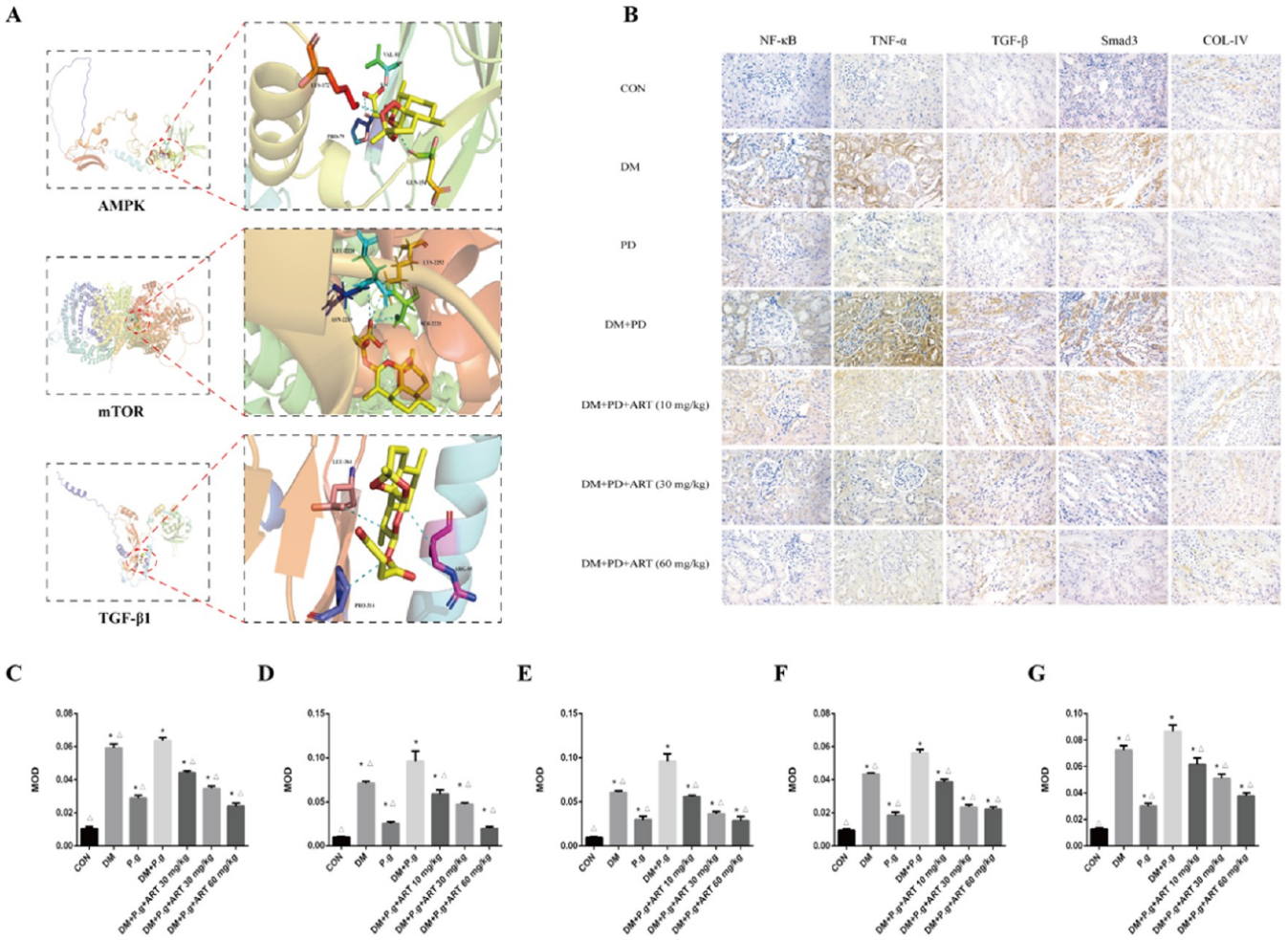

Figure 6. Type 1 diabetes with periodontitis induced renal injury via the TGF-β/Smad signaling pathway. (A) Protein−ligand interactions and molecular dynamics analysis of ART with AMPK, mTOR, and TGF-β. (B) Immunohistochemical staining of NF-κB, TNF-α, TGF-β, Smad3, and COL-IV for the kidney tissue (200×). (C−G) Gray-scale bar graph of immunohistochemistry. *P < 0.05, the results of each group were compared with the CON group. $^{\Delta}P$ < 0.05, the results of each group were compared with the DM + PD group.

amplification was performed only after the purity of the extract was tested and conformity was determined. Libraries were constructed based on purified products using Ion Plus Fragment Library Kit 48 rxns (Thermo Fisher). The library constructed above was checked to be qualified, and then Ion S5TMXL from Thermo Fisher was used for sequencing.

2.13. Statistical Analysis. A one-way analysis of variance (ANOVA) was used to examine differences among seven groups, followed by a least significant difference post hoc test to identify the least significant difference. Statistical analysis was performed using SPSS v22.0 software (IBM Corp.), with a P value of 0.05 considered statistically significant.

3. RESULTS

3.1. Establishment of Animal Models. We established rat models with type 1 diabetes and periodontitis. In the pathological observation of periodontal tissue, H&E staining showed that the arrangement of collagen fibers in the PD group was disordered, and inflammatory cells were scattered. The methylene blue staining result suggested that there were active osteocloblastic lacunae in the PD group. We also observed a decrease in cortical bone, cancellous bone, and total bone mineral density in PD by performing micro-CT (Figure 1A,D). The immunohistochemical results of periodontal tissues showed that the positive rate of TNF-α and RANKL was higher in the PD group, while OPG did not show that in the PD group (Figure 2A). The pathological conditions described above were more serious in the DM + PD group. For the diabetic model, after 8 weeks of modeling, rats showed excessive drinking, eating, urination, and weight loss, but the general conditions of the rats were poor with dry fur, low mobility, and microalbuminuria. In addition to dark red free gingiva that was occasionally swollen and bleeding, rats in the DM group had worse oral hygiene than rats in the CON group. In terms of biochemical data, the expression levels of Scr, BUN, U-TP, β2-MG, UA, FBG, and Cysc were significantly higher in the DM and DM + PD groups than in the CON group (Figure 3). In conclusion, the above results indicate that the rat model was successfully established.

3.2. Periodontal Disease Aggravates the Fibrosis of Diabetic Nephropathy by Inducing Autophagy and Pathway. Our immunohistochemistry results showed that the expression of NF-κB and TNF-α in kidney tissue of the PD group was higher than that in the CON group. Compared with nondiabetic rats (the CON and PD group), the expressions of AMPK and LC3-II in diabetic rats (the DM and DM + PD group) were significantly decreased, while mTOR and P62 were significantly increased. Additionally, compared with

https://doi.org/10.1021/acsomega.4c00020
ACS Omega 2024, 9, 16358−16373

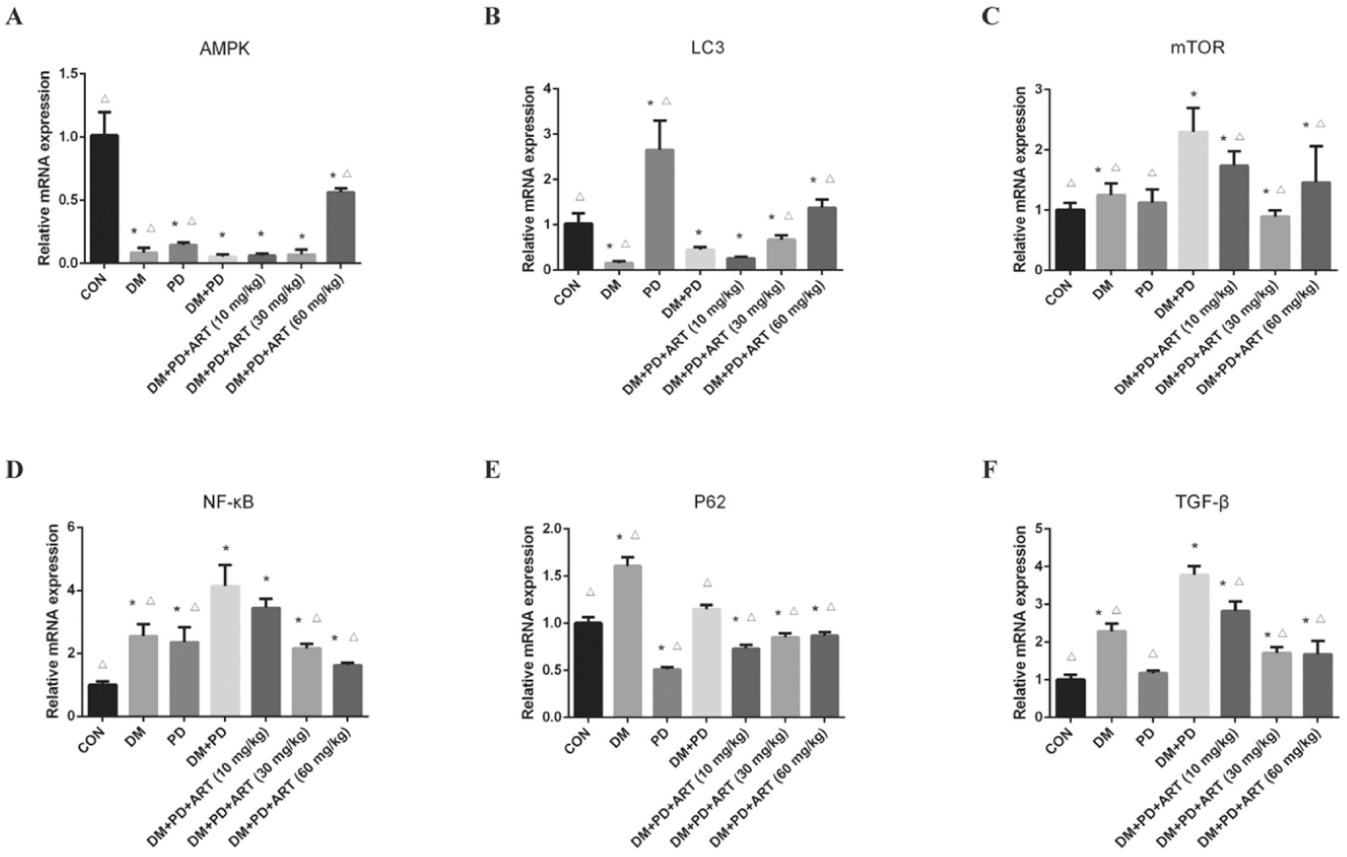

Figure 7. AMPK (A), LC3 (B), mTOR (C), NF-κB (D), P62 (E), TGF-β (F) mRNA expression in kidney tissue of rats in each group. *$P < 0.05$, the results of each group were compared with the CON group. $^{\Delta}P < 0.05$, the results of each group were compared with the DM + PD group.

nondiabetic rats (the CON and PD group), the expressions of NF-κB and TNF-α in diabetic rats (the DM and DM + PD group) were increased. The expression of fibrosis-related proteins TGF-β, Smad3, and COL-IV in diabetic rats (the DM and DM + PD group) was enhanced. The above pathological changes in the DM + PD group were more obvious than those in the DM group. These results were further confirmed by RT-PCR and Western blot.

3.3. ART Reduces Renal Fibrosis by Increasing the Level of Autophagy. After ART intervention, H&E staining showed that the reticular fibers were arranged neatly and the infiltration of inflammatory cells was reduced in the periodontal tissue of rats with periodontal disease. Methylene blue staining also showed that the reduction of bone resorption lacunae in the cortical bone was more significant in the 60 mg/kg group than in the 10/30 mg/kg group (Figure 1A). In terms of bone resorption, the 60 mg/kg group improved more significantly than the 10/30 mg/kg group (Figure 1D). In immunohistochemistry, the situation of TNF-α, OPG, and RANKL was improved, and the effect increased in a dose-dependent manner (Figure 2).

In the kidney tissue, H&E, PAS, and Masson staining showed that the pathological changes of renal fibrosis were relieved after ART intervention (Figure 4A). The expressions of inflammatory factors NF-κB and TNF-α and fibrosis-related factors TGF-β, Smad3, and COL-IV were reduced (Figure 6A). About autophagy-related factors, AMPK, mTOR, P62, and LC3-II were improved (Figure 5A,B). The number of terminal deoxynucleotidyl transferase dUTP nick end labeling (TUNEL)-positive cells was also reduced (Figure 4B). However, among the three concentration groups, 60 mg/kg had the best outcome (Figure 6). Finally, PCR and WB results further supported the above results (Figures 7 and 8).

3.4. Oral Flora Is Associated with the Progression of Kidney Injury. To investigate the interaction between periodontal and renal microflora, we performed 16S sequencing analysis on saliva samples in each group, and the result showed that the CON group, PD group, DM group, and DM + PD group had 111, 243, 130, and 216 unique OTUs, respectively. In kidney tissue, compared with the CON group, 4 OTUs were unique to the PD group, and 6 OTUs were unique to the DM + PD group (Figure 9). This result suggested that P. gingivalis may affect the renal flora, but the result was not significant, which may be related to the insufficient sample size.

After ART intervention, 17 OTUs were found to be unique to the DM + PD + ART (30 mg/kg) group, and 4 OTUs were unique to the DM + PD + ART (60 mg/kg) group, indicating a decrease in the number of OTUs. In kidney tissue, the number of OTUs increased after ART intervention, and the microflora changed significantly in the 60 mg/kg group. The above results suggested that ART may affect the diversity of microflora in the oral cavity and kidneys, and 60 mg/kg ART treatment may change the internal environment of the body and affect the reproduction of microflora.

In the analysis of species composition, a total of 17 bacterial phyla were detected in the kidney tissues from 7 groups of samples. At the Phylum level, the top 5 most abundant phyla were Proteus, Firmicutes, Bacteroides, Actinomyces, and Fusobacterium. The dominant phyla in the gingival crevicular

https://doi.org/10.1021/acsomega.4c00020
ACS Omega 2024, 9, 16358−16373

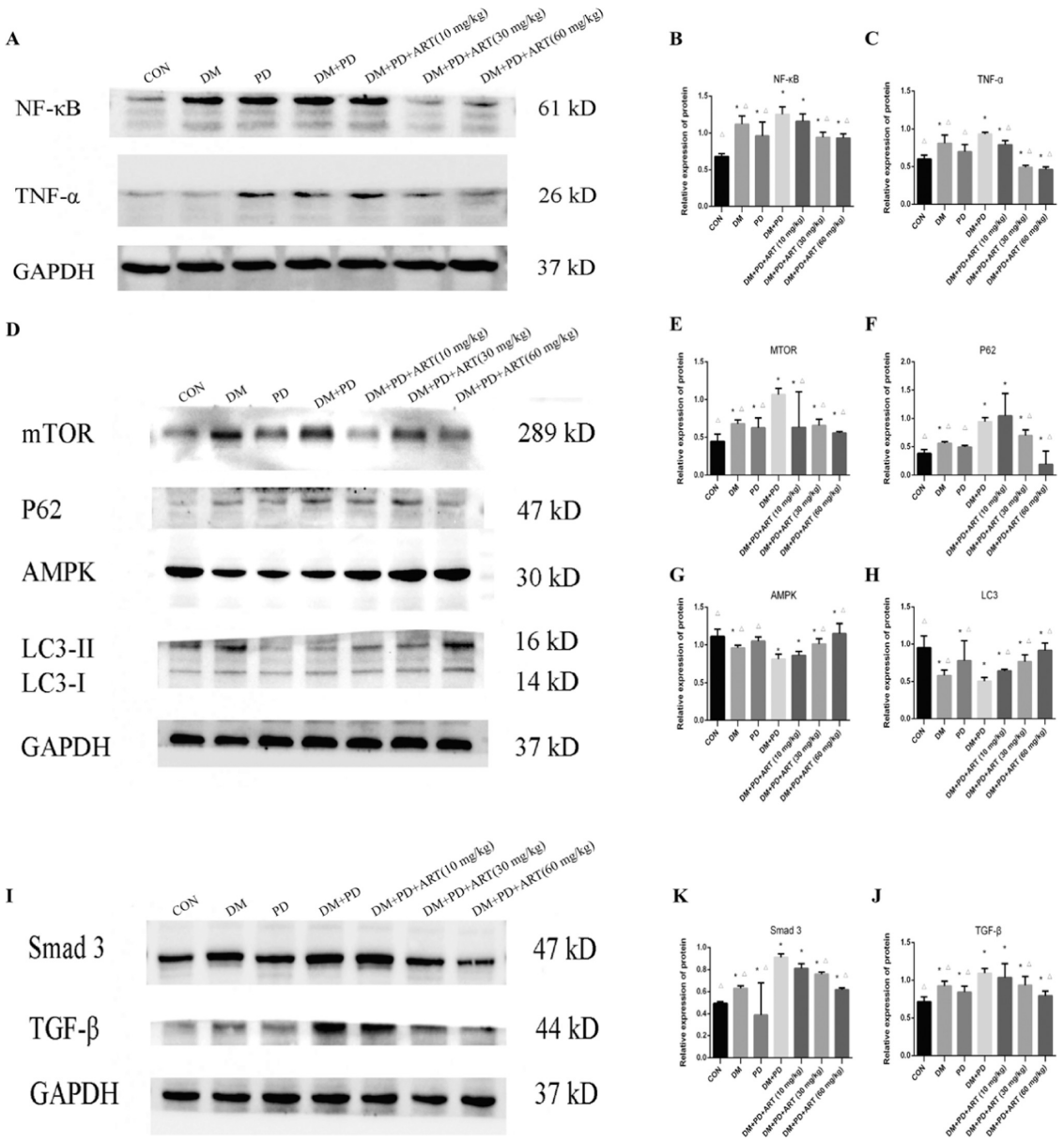

Figure 8. Western Blot results showed that autophagy mediated kidney damage. (A) Results of Western blot assay for the inflammatory factor NF-κB and TNF-α. (B, C) Gray-scale bar plots of NF-κB and TNF-α protein expression. (D) Western blot results of autophagy-related factors. (E−H) Gray-scale bar plots of mTOR, P62, AMPK, and LC3 protein expression. (I) Western blot results of fibrosis-related factors. (J, K) Gray-scale bar plots of Smad2 and TGF-β protein expression. $^{*}P < 0.05$, the results of each group were compared with the CON group. $^{\Delta}P < 0.05$, the results of each group were compared with the DM + PD group.

fluid of each sample are shown in Figure 10; compared to the CON group, the proportion of Proteobacteria and Firmicutes in the DM, PD, and DM + PD groups increased. After ART intervention, compared to the DM + PD group, the abundance of Proteobacteria was decreased, and the proportions of Bacteroidetes and Firmicutes were significantly reduced. The proportion of Proteobacteria in the DM + PD + ART (60 mg/kg) group showed a significant downward trend.

The distribution of bacterial flora in the kidneys was roughly the same as that in the oral cavity, suggesting that ART has the same regulatory effect on the flora of various organs and may inhibit the proliferation of some bacterial flora. After ART intervention, the diversity of microbiota in both groups decreased; in the kidney, the diversity of microbiota in the DM + PD + ART (30 mg/kg) group was close to that in the CON group, and the diversity of microbiota in the DM + PD + ART (60 mg/kg) group decreased.

4. DISCUSSION

With the continuous update of the understanding of the pathogenesis of DKD, renal tubular injury is still considered to be an important link in the occurrence of DKD. Podocyte loss, mesangial expansion, and reduced capillary surface are the main features of DKD.[25] In addition, clinical evidence has shown that the renal tubules of patients with diabetes also exhibit interstitial fibrosis, tubular atrophy, and peritubular capillary rarefication.[26] The proximal tubule is responsible for the heavy absorption process; this is a kind of active transport process, which requires a lot of energy, making the kidneys to oxygen demand. Renal tubular epithelial cells in the diabetic

https://doi.org/10.1021/acsomega.4c00020
ACS Omega 2024, 9, 16358−16373

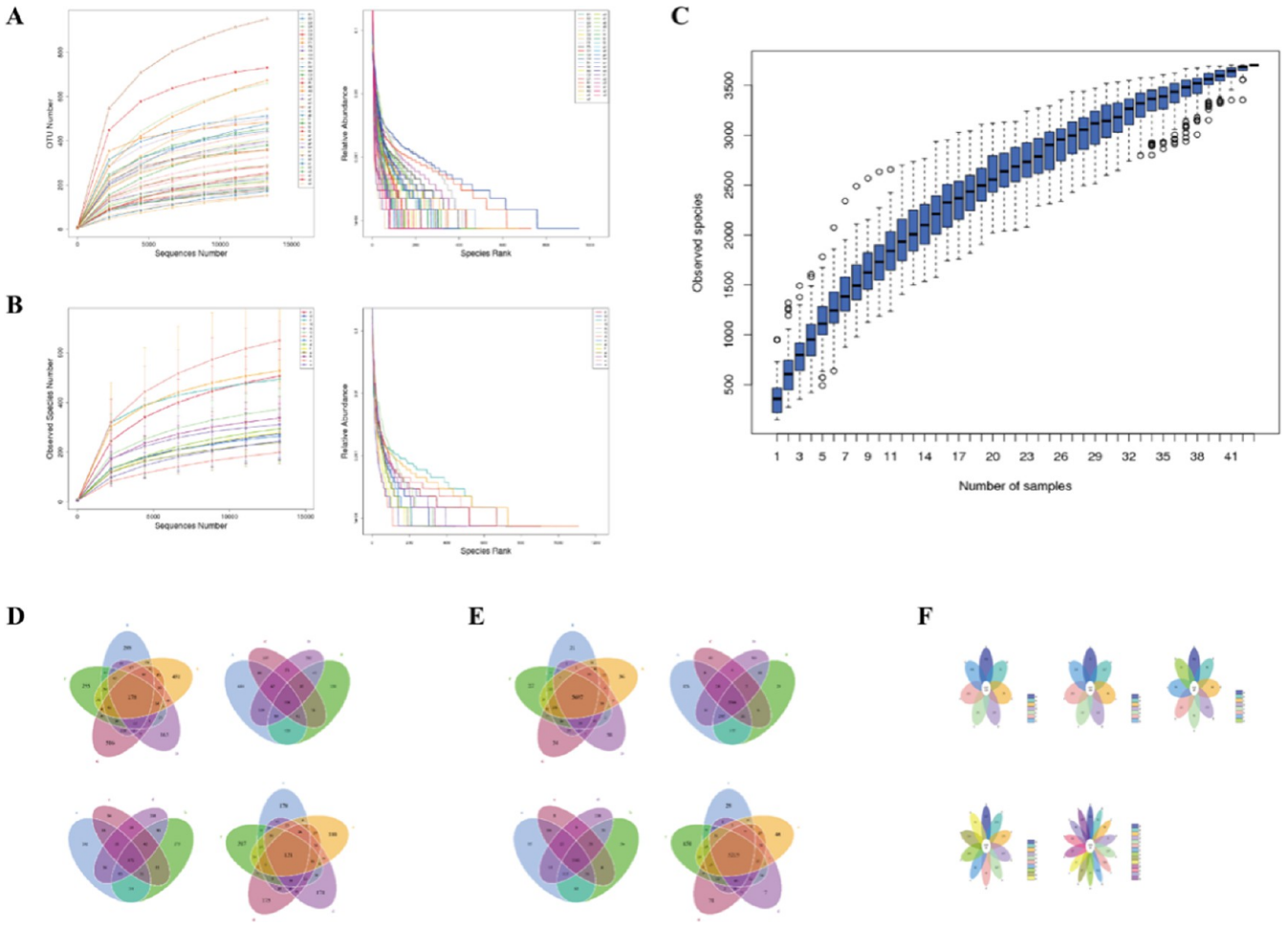

Figure 9. Experimental Results of 16S sequencing. (A, B) Rank abundance curve in oral flora and kidney flora. (C) Species accumulation boxplot. (D−F) OTU flower and Venn diagrams of oral flora and kidney flora in rats. A(kidney)/a(oral swabs): CON group. B(kidney)/b(oral swabs): DM group. C(kidney)/c(oral swabs): PD group. D(kidney)/d(oral swabs): DM + PD group. E(kidney)/e(oral swabs): DM + PD + ART (10 mg/kg) group. F(kidney)/f(oral swabs): DM + PD + ART (30 mg/kg) group. G(kidney)/g(oral swabs). DM + PD + ART (60 mg/kg) group.

state are particularly sensitive to the disease due to their dependence on aerobic metabolism and high energy demand.[27] Kidney pathological changes such as renal tubular cell apoptosis, renal tubular necrosis, the transformation of epithelial-mesenchymal and ECM deposition, etc., can be caused by hyperglycemia independently.[28] In addition, due to the glucose metabolism disorder caused by the hyperglycemic state, the burden of glucose reabsorption in the proximal tubule increases, leading to tubular hypertrophy and a large amount of reactive oxygen species production. These burdens lead to G1 cell cycle arrest and senescence phenotypes in proximal tubular cells that promote interstitial inflammation and fibrosis.[27,28] Recent studies have shown that systemic low inflammation induced by hyperglycemia induces macrophages to secrete senescence-related secretory phenotype components, which further promotes the escalation of inflammation in kidney tissue, and finally directly induces senescence of renal tubular epithelial cells and mesangial cells.[29,30] Mechanistically, it may be that the accumulation of damaged mitochondria leads to premature cellular senescence. First, high blood sugar in the body state offers help to the microenvironment of cell aging. Second, telomere shortening due to oxidative stress may be the most critical. As protectors of genome integrity, telomere inactivation or shortening can initiate DNA double-strand breaks and eventually lead to premature cellular senescence.[31,32] Apoptosis of renal tubular epithelial cells is also a major feature of DKD. In vivo and in vitro evidence that high blood sugar caused renal tubule cells to produce free radicals and oxidative stress improves the rate of apoptosis.[33] In addition, the ROS produced promoted the progression of renal fibrosis through the activation of apoptosis signal-regulated kinase 1, which in turn activated the downstream p38 mitogen-activated protein kinase (MAPK).[34] Ferroptosis is a newly reported regulated cell death (RCD). Excessive ROS production due to iron accumulation in cells disrupts the stability of cell functions and eventually drives cells toward death.[35] As a key regulator of ferroptosis, GPX4 inactivation will cause lipid peroxide accumulation and eventually trigger ferroptosis.[36] Recent animal experimental studies show that GPX4 defect of proteinuria and renal interstitial edema in mice and renal tubular cell death were significantly increased, prompting GPX4 cells of renal tubules with renin protection. Combined with clinical evidence from diabetic kidney biopsy samples, GPX4 mRNA expression is significantly reduced compared to non-diabetic patients, and ferroptosis can be considered a form of tubular cell death.[37] Pyroptosis belonging to RCD has proven to participate in renal tubular cell death.[38] Pyroptosis by protease dependency GSDMD cutting is a congenital immune response to pathogens in the cell. In the process of apoptosis, GSDMD cutting segments of the

https://doi.org/10.1021/acsomega.4c00020
ACS Omega 2024, 9, 16358−16373

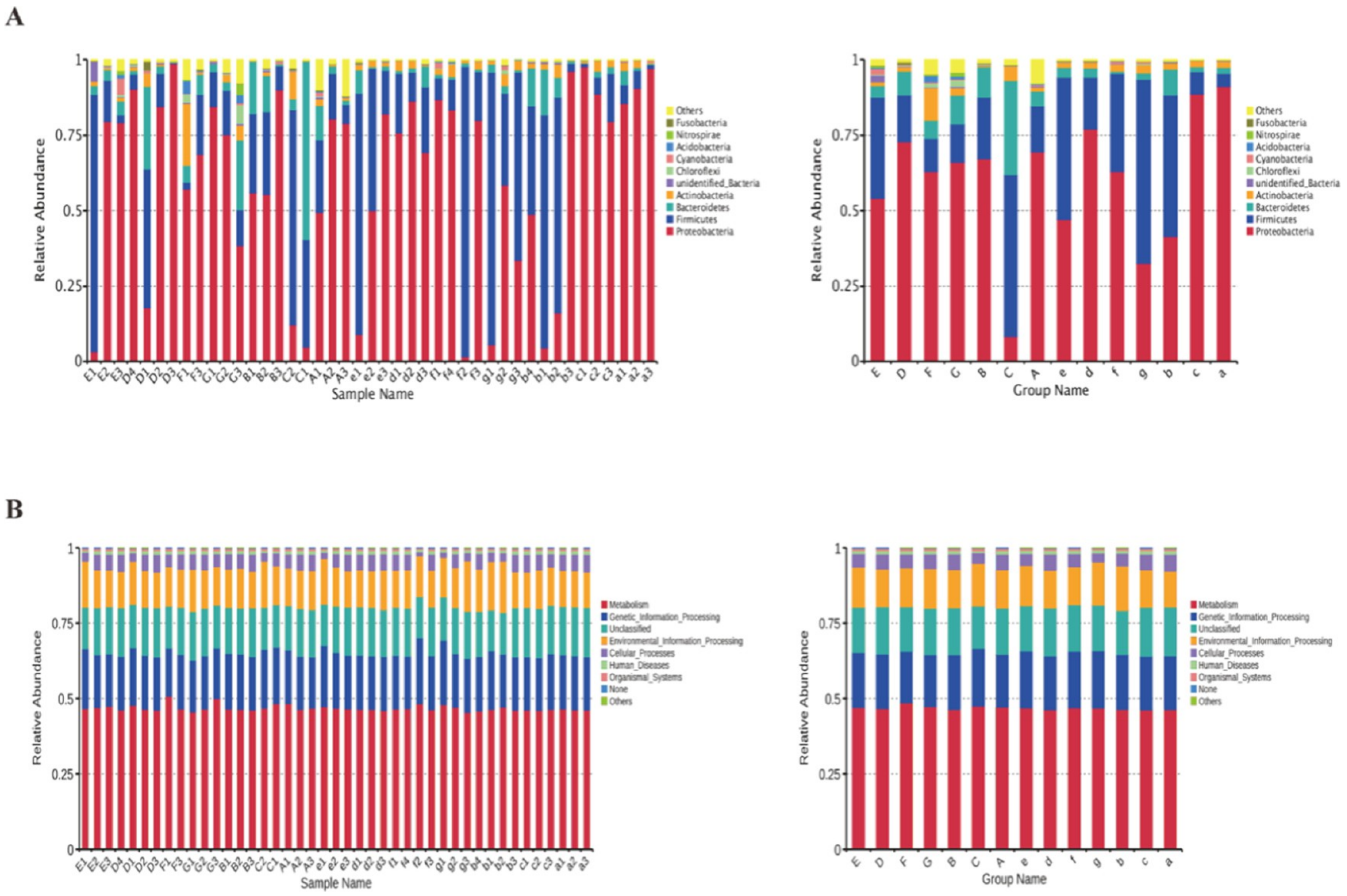

Figure 10. Taxonomic composition analysis of oral microflora individuals and intergroups and kidney microflora individuals and intergroups in rats. A(kidney)/a(oral swabs): CON group. B(kidney)/b(oral swabs): DM group. C(kidney)/c(oral swabs): PD group. D(kidney)/d(oral swabs): DM + PD group. E(kidney)/e(oral swabs): DM + PD + ART (10 mg/kg) group. F(kidney)/f(oral swabs): DM + PD + ART (30 mg/kg) group. G(kidney)/g(oral swabs). DM + PD + ART (60 mg/kg) group.

Table 1. Primers Sequences of Target Genes and Reference Genes

gene	forward primer	reverse primer
β-actin	GGAGATTACTGCCCTGGCTCCTA	GACTCATCGTACTCCTGCTTGCTG
NF-κB	GGCAGCACTCCTTATCAAC	GGTGTCGTCCCATCGTAG
TGF-β	ACGTCAGACATTCGGGAAGCAGTG	GCAAGGACCTTGCTGTACTGTACT
AMPK	TTCTGTCTGCCGTGGACTACT	CAGCCTTCCTGAGATGACCT
mTOR	CCAGGAAATACCCTCTCTCCATC	GAAGGTCACAAAGCCGTCTT
LC3-II	CGAACAAAGAGTGGAAGATGTC	AGGCTTGGTTAGCATTGAGC
P62	AGCTGCCCTCAGCCCTCT	GGCTTCTCTTCCCTCC

formation of amino-terminal permeation membrane and membrane pore formation promote the IL-1β, IL-18 the release of inflammatory factors, etc.[39] NLRP3, as a potent mediator of inflammation, can activate IL-1β, IL-18, and caspase-1.[40] It has been reported that hyperglycemia, hyperuricemia, and hyperlipidemia can activate NLRP3 to cause pyroptosis.[41] Clinical data show that the NLRP3 inflammasome is also activated in some intrinsic renal cells (renal tubular epithelial cells) of renal patients. Experiments in mice suggested that IL-1β and IL-18 were produced by renal tubular epithelial cells.[40]

Autophagy is a specific cell death pathway. Responsible for autophagosome initiation, formation, and maturation is the family of autophagy-related genes. The occurrence of autophagy can be summarized as autophagy body fusion with lysosomes, and degradation by autophagy hydrolysis/package material.[42] mTOR and AMPK are the major regulatory proteins of the autophagy process.[43] Reports show that autophagy in diabetic patients may be caused by high glucose because the high glucose state induces the accumulation of dysfunctional organelles and unfolded proteins in the cells. Thus, the development of TGF-β-regulated fibrosis and renal cell injury can be caused by the blockage of the process of clearance of damaged cell contents.[44] In DKD, Smad3-enabled triggering autophagic dysfunction is promoting factors of disease progression. The possible mechanism is that Smad3 binds and represses TFEB expression at the transcriptional level, inhibiting lysosome formation and hindering the clearance of damaged lysosomes, leading to lysosomal depletion in renal tubular epithelial cells during diabetes.[45] In our work, Smad3 was highly expressed in the DM group and the DM + PD group, which was more significant in the DM +

https://doi.org/10.1021/acsomega.4c00020
ACS Omega 2024, 9, 16358−16373

PD group, suggesting that periodontitis aggravated the autophagy dysfunction triggered by Smad3 in the kidney tissue. After ART intervention, the expression of Smad3 showed a downward trend, and 60 mg/kg ART had the best effect, suggesting that ART can protect the stability of autophagy by inhibiting the activation of Smad3.

AMPK is an important energy sensor, which can regulate the body's energy metabolism, induce apoptosis, improve inflammation, regulate oxidative stress, and promote autophagy.[46,47] Therefore, inhibition of AMPK can aggravate the occurrence and development of renal fibrosis, and AMPK activation can inhibit renal fibrosis.[48−50] The inflammatory response involved in inflammatory cytokines/cells promotes the process from repair response to injury in the kidney, and the persistent inflammatory response accelerates the process of renal fibrosis.[2,38,,52] TNF-α can affect the morphology and skeleton of mesangial cells and stimulate the proliferation of mesangial cells and the proliferation of fibroblasts, which are the main protein source of ECM.[53,54] IL-1β induces an inflammatory response and stimulates the synthesis and secretion of TNF-α, which synergistically promotes the development of renal fibrosis. NF-κB is a regulatory factor of inflammation and immune response, closely related to DN's occurrence and development.[55,56] Under high glucose conditions, NF-κB accumulates in the cytoplasm, leading to a large amount of inflammation in the kidney tissue and causing glomerular and renal interstitial fibrosis. The NF-κB signaling pathway can participate in the pathophysiology and renal interstitial fibrosis of early DN through a variety of mechanisms.[55,57] In addition, activated AMPK can also block the NF-κB signaling pathway, improve the blood glucose level of diabetic rats, reduce the expression of pro-inflammatory factors, and play an anti-inflammatory role.[58,59] Therefore, we hypothesized that AMPK may aggravate kidney injury in type 1 diabetic rats with periodontal disease by regulating the TGF-β and NF-κB signaling pathways. The results of this experiment showed that the contents of NF-κB, TNF-α, TGF-β1, and COL-IV in the PD group were higher than those in the CON group. It is suggested that periodontal disease may aggravate renal inflammation and cause renal fibrosis. The expressions of AMPK and LC3-II in the DM group and the DM + PD group were significantly decreased; the expressions of mTOR and P62 proteins were increased; the expressions of inflammatory factors NF-κB and TNF-α were increased; and the expressions of fibrosis proteins TGF-β, Smad3, and COL-IV were increased. The changes in the DM + PD group were more obvious than those in the DM group. These results suggest that diabetes impairs renal function in rats and periodontal disease may aggravate the impairment of renal function in diabetic rats.

To further confirm our hypothesis, based on the above experimental results, molecular docking and molecular dynamics were used to analyze the binding site of ART with AMPK, mTOR, and TGF-β. The molecular docking simulation of ART and each protein showed that the binding energy of each protein to ART was less than 0 in the initial screening results, indicating that ART and each protein could naturally combine, which was of research value. ART has a strong binding ability with AMPK and mTOR, among which mTOR has the highest score with the optimal binding energy of −8.0 kcal/mol, while AMPK and TGF-β have a lower binding energy with the optimal conformation of −6.30 and −6.20 kcal/mol, respectively. As shown in the Figure 6, ART forms hydrophobic interactions with amino acid residues LEU-2220, SER-2221, LYS-2252, and ASN-2219 in the active site of mTOR chain. These forces enable ART to firmly bind to the active site of mTOR. In addition, ART binds to amino acid residues VAL-81, PRO-79, GLN-154, and LYS-172 in the active site of the AMPK chain through hydrophobic interaction.

Based on "gut−kidney axis" theory to study, the strategy of prevention and treatment of kidney diseases draw increasing attention, and kidney disease is mainly involved in chronic kidney diseases such as DKD.[60,61] Kidney in the activation of the renin-angiotensin system (RAS) of DKD is a key factor in the present study that the intestinal flora can activate the system. Studies have found that the plasma acetate level is decreased, the activation of intrarenal RAS is inhibited, and renal damage is alleviated after the intervention of compound broad-spectrum antibiotics in diabetic rats, suggesting that excessive acetate produced by intestinal flora imbalance may cause early renal damage by activating intrarenal RAS.[62] In the condition of diabetes, the accumulation of succinic acid salt with G protein-coupled receptors and activation of renal RAS, eventually cause DKD.[63] As gut microbes' glycolysis carbohydrate metabolic product, short-chain fatty acids (SCFAs) is considered anti-inflammatory, antibacterial, anti-fibrosis, resistant to oxidative stress, and regulation of autophagy and renal protection effect.[64] After sodium butyrate intervention, the levels of butyrate in serum and feces of diabetic rats are increased, and the renal damage is alleviated.[65] Primary bile acids are converted into secondary bile acids by Firmicutes organisms in the gut, and Lactobacillus, Bacteroides, and Roseobacter are involved in this metabolic process.[66] Animal studies suggest that it can be triggered by the secondary bile acid method, farnesoid X receptor (FXR), and G protein coupling bile acid receptor 1 (TGR5) and alleviate kidney inflammation, oxidative stress, and renal fibrosis.[67] Indoxyl sulfate (lS) and *p*-cresyl sulfate (PCS), produced by intestinal microbial fermentation of aromatic amino acids, are the most important enterogenous uremic toxins.[68] In addition, intestinal microorganisms metabolize nutrients, such as choline and carnitine, in food to produce trimethylamine. It is then metabolized by the liver to produce trimethylamine N-oxide (TMAO). In the DKD state, increased levels of these enterogenous uremic toxins can increase intestinal permeability, stimulate the immune system, induce glomerular and tubular damage, and perpetuate inflammation, oxidative stress, and fibrosis.[69] Many studies have shown that inflammatory response is involved in the occurrence and development of DKD.[70] In the diabetic state, the relative abundance of butyrate-producing gut bacteria is reduced, and the corresponding reduction of SCFAs and hyperglycemia itself can lead to increased intestinal permeability and LPS translocation. LPS entering the blood circulation can induce inflammatory responses by binding to Tol-like receptor 4 in the kidney.[71] In the state of DKD, the accumulation of enterogenous uremic toxins can aggravate the inflammatory response and worsen the renal function. IS and PCS have been confirmed to have a strong pro-inflammatory effect. IS and PCS can activate intrarenal RAS and induce renal fibrosis.[72] Angiotensin-converting enzyme (ACE) and angiotensin-converting enzyme 2 (ACE2) are important regulators of RAS under normal conditions. The balance of ACE and ACE2 was maintained in the kidney. In a diabetic state, intestinal flora imbalance may be involved in the occurrence and

https://doi.org/10.1021/acsomega.4c00020
ACS Omega 2024, 9, 16358−16373

development of DKD by breaking the balance of ACE and ACE2 in the kidney.[73] The dysbiosis of intestinal flora caused by periodontal disease has been demonstrated by a large amount of evidence.[74] In the present study, periodontal disease showed an effect of accelerating DN, and the possible mechanism is that the intestinal flora imbalance caused by oral flora imbalance disrupts the intrarenal ACE/ACE2 balance. The subsequent intestinal metabolic disorders further aggravate this process. After analyzing the 16S rDNA genome sequencing results, we found that compared with the DM + PD group, the DM + PD + ART (10 mg/kg), DM + PD + ART (30 mg/kg), and DM + PD + ART (60 mg/kg) groups had significant changes in oral flora. The level of oral microbiota in the DM + PD + ART (30 mg/kg) group was similar to that in the CON group. Therefore, ART may indirectly regulate intestinal flora by regulating the balance of oral flora, restoring the normal metabolism of intestinal flora, and then improving renal lesions. But ART adjusts the specific mechanisms of oral flora; an extreme effect on the intestinal flora also needs further experiments to confirm.

5. CONCLUSIONS

In order to determine the impact of periodontal disease on the progression of renal damage in the diabetic state and to find the appropriate medical treatment for this complication, we designed and implemented this study work. Our work suggests that periodontal disease may mediate the imbalance of renal flora, aggravate renal damage in type 1 diabetes, cause glomerular inflammation and renal tubulointerstitial fibrosis, and reduce autophagy. However, ART intervention can regulate the periodontal flora, reduce the expression of TNF-α, OPG, RANKL, and alkaline phosphatase (ALP) in gingival tissue, reduce alveolar bone loss, and restore bone tissue reconstruction. In addition, a certain dose of ART can promote the recovery of bacterial flora to normal levels, reduce renal inflammation, inhibit renal fibrosis, and improve the level of autophagy to delay kidney injury.

■ ASSOCIATED CONTENT

Data Availability Statement

The data that support the findings of this study are openly available.

■ AUTHOR INFORMATION

Corresponding Author

Xiaolin Nong − *College of Stomatology, Hospital of Stomatology, Guangxi Medical University, Nanning 530021 Guangxi, China; Guangxi Key Laboratory of Oral and Maxillofacial Rehabilitation and Reconstruction, Guangxi Medical University, Nanning 530021 Guangxi, China*; Email: xnong@gxmu.edu.cn

Authors

Chen Liang − *College of Stomatology, Hospital of Stomatology, Guangxi Medical University, Nanning 530021 Guangxi, China*; orcid.org/0000-0001-9315-6917

Licheng Ma − *College of Stomatology, Hospital of Stomatology, Guangxi Medical University, Nanning 530021 Guangxi, China*

Yi Chen − *College of Stomatology, Hospital of Stomatology, Guangxi Medical University, Nanning 530021 Guangxi, China*

Jiaquan Li − *Medical Science Research Center, Guangxi Medical University, Nanning 530021 Guangxi, China*

Binge Wang − *College of Stomatology, Hospital of Stomatology, Guangxi Medical University, Nanning 530021 Guangxi, China*

Chubin Ma − *College of Stomatology, Hospital of Stomatology, Guangxi Medical University, Nanning 530021 Guangxi, China*

Zhong Yuan − *College of Stomatology, Hospital of Stomatology, Guangxi Medical University, Nanning 530021 Guangxi, China*

Complete contact information is available at: https://pubs.acs.org/10.1021/acsomega.4c00020

Author Contributions

‖C.L. and L.M. contributed equally to this work. C.L. and X.N. conceived the experiments,designed the study, and wrote the manuscript. C.L., L.M., Y.C., J.L., B.W., C.M., and Z.Y. performed experiments. C.L. and L.M. analyzed the data. All authors read and approved the final manuscript.

Funding

The present study was supported by research grants from the National Nature Science Foundation of China (81860726), the Natural Science Foundation Key Project of Guangxi (2019GXNSFDA245016), and the Guangxi Medical and Health Appropriate Technology Development and Promotion Application Project (S2019059). The funder had no role in the study design; the collection, analysis, and interpretation of the data; or in the writing of the manuscript.

Notes

The authors declare no competing financial interest.

All animal experiments were approved by the Animal Care & Welfare Committee of Guangxi Medical University (ethics number: 201808310), Nanning, Guangxi, China, and investigations conformed to Guiding Opinions on the Good Treatment of Experimental Animals issued by the Ministry of Science and Technology of the People's Republic of China and the National standard GB/T35892-2018 Guidelines for Ethical Review of Experimental Animal Welfare of the People's Republic of China

■ ACKNOWLEDGMENTS

The authors are grateful for the financial support from NSFC and all the members of the research group who participated in the study.

■ ABBREVIATIONS

ALP	alkaline phosphatase
AMPK	AMP-activated protein kinase
ART	artesunate
BMP-7	bone morphogenetic protein 7
BUN	blood urea nitrogen
Cysc	cystatin C
COL-IV	collage type IV
CKD	chronic kidney disease
DM	diabetes mellitus
DKD	diabetic kidney disease
ECM	extracellular matrix
FBG	fasting blood glucose
FPS	fucoidan
IL-1β	interleukin-1β
LPS	lipopolysaccharide

https://doi.org/10.1021/acsomega.4c00020
ACS Omega 2024, 9, 16358−16373

mTOR	mammalian protein of rapamycin
NF-κB	nuclear factor-κB
OPG	osteoprotegerin
PAI-1	plasminogen activator inhibitor-1
PD	periodontal disease
RANKL	receptor activator of NF-κB ligand
Scr	serum creatinine
Smad3	Sma and Mad homologue
STZ	streptozotocin
TGF-β	transforming growth factor-β
TNF-α	tumor necrosis factor-α
T1DM	type 1 diabetes mellitus
UA	uric acid
β2-MG	beta2 microglobulins

REFERENCES

(1) Adler, S.; Nast, C.; Artishevsky, A. Diabetic Nephropathy: Pathogenesis and Treatment. *Annu. Rev. Med.* **1993**, *44* (1), 303−315.

(2) Wada, J.; Makino, H. Inflammation and the Pathogenesis of Diabetic Nephropathy. *Clin. Sci.* **2013**, *124* (3), 139−152.

(3) Glickman, I. Periodontal Disease. *N. Engl. J. Med.* **1971**, *284* (19), 1071−1077.

(4) Ioannidou, E.; Hall, Y.; Swede, H.; Himmelfarb, J. Periodontitis Associated with Chronic Kidney Disease among Mexican Americans. *J. Public Health Dent.* **2013**, *73* (2), 112−119.

(5) Wahid, A.; Chaudhry, S.; Ehsan, A.; Butt, S.; Kahn, A. A. Bidirectional Relationship between Chronic Kidney Disease & Periodontal Disease: A Review. *Pak. J. Med. Sci.* **2012**, *29* (1), No. 211, DOI: 10.12669/pjms.291.2926.

(6) Sawa, Y.; Takata, S.; Hatakeyama, Y.; Ishikawa, H.; Tsuruga, E. Expression of Toll-Like Receptor 2 in Glomerular Endothelial Cells and Promotion of Diabetic Nephropathy by Porphyromonas Gingivalis Lipopolysaccharide. *PLoS One* **2014**, *9* (5), No. e97165.

(7) Fang, F.; Wu, B.; Qu, Q.; Gao, J.; Yan, W.; Huang, X.; Ma, D.; Yue, J.; Chen, T.; Liu, F.; Liu, Y. The Clinical Response and Systemic Effects of Non-Surgical Periodontal Therapy in End-Stage Renal Disease Patients: A 6-Month Randomized Controlled Clinical Trial. *J. Clin. Periodontol.* **2015**, *42* (6), 537−546.

(8) Deschamps-Lenhardt, S.; Martin-Cabezas, R.; Hannedouche, T.; Huck, O. Association between Periodontitis and Chronic Kidney Disease: Systematic Review and Meta-Analysis. *Oral Dis.* **2019**, *25* (2), 385−402.

(9) Hwang, H.-Y.; Shim, J. S.; Kim, D.; Kwon, H. J. Antidepressant Drug Sertraline Modulates AMPK-MTOR Signaling-Mediated Autophagy via Targeting Mitochondrial VDAC1 Protein. *Autophagy* **2021**, *17* (10), 2783−2799.

(10) Lin, C.; Zhang, M.; Zhang, Y.; Yang, K.; Hu, J.; Si, R.; Zhang, G.; Gao, B.; Li, X.; Xu, C.; Li, C.; Hao, Q.; Guo, W. Helix B Surface Peptide Attenuates Diabetic Cardiomyopathy via AMPK-Dependent Autophagy. *Biochem. Biophys. Res. Commun.* **2017**, *482* (4), 665−671.

(11) Bhargava, P.; Schnellmann, R. G. Mitochondrial Energetics in the Kidney. *Nat. Rev. Nephrol.* **2017**, *13* (10), 629−646.

(12) Tang, G.; Li, S.; Zhang, C.; Chen, H.; Wang, N.; Feng, Y. Clinical Efficacies, Underlying Mechanisms and Molecular Targets of Chinese Medicines for Diabetic Nephropathy Treatment and Management. *Acta Pharm. Sin. B* **2021**, *11* (9), 2749−2767.

(13) Chen, K.; Yu, B.; Liao, J. LncRNA SOX2OT Alleviates Mesangial Cell Proliferation and Fibrosis in Diabetic Nephropathy via Akt/MTOR-Mediated Autophagy. *Mol. Med.* **2021**, *27* (1), 71.

(14) Ha, H.; Lee, H. B. Reactive Oxygen Species and Matrix Remodeling in Diabetic Kidney. *J. Am. Soc. Nephrol.* **2003**, *14* (3), S246−S249.

(15) Kanwar, Y. S.; Sun, L.; Xie, P.; Liu, F.; Chen, S. A Glimpse of Various Pathogenetic Mechanisms of Diabetic Nephropathy. *Annu. Rev. Pathol.: Mech. Dis.* **2011**, *6* (1), 395−423.

(16) Wang, L.; Wang, H.-L.; Liu, T.-T.; Lan, H.-Y. TGF-Beta as a Master Regulator of Diabetic Nephropathy. *Int. J. Mol. Sci.* **2021**, *22* (15), 7881.

(17) Gifford, C. C.; Tang, J.; Costello, A.; Khakoo, N. S.; Nguyen, T. Q.; Goldschmeding, R.; Higgins, P. J.; Samarakoon, R. Negative Regulators of TGF-B1 Signaling in Renal Fibrosis; Pathological Mechanisms and Novel Therapeutic Opportunities. *Clin. Sci.* **2021**, *135* (2), 275−303.

(18) Kitada, M.; Ogura, Y.; Monno, I.; Koya, D. Regulating Autophagy as a Therapeutic Target for Diabetic Nephropathy. *Curr. Diabetes Rep.* **2017**, *17* (7), 53.

(19) Xu, J.; Liu, L.; Xu, L.; Xing, Y.; Ye, S. Metformin Alleviates Renal Injury in Diabetic Rats by Inducing Sirt1/FoxO1 Autophagic Signal Axis. *Clin. Exp. Pharmacol. Physiol.* **2020**, *47* (4), 599−608.

(20) Ma, N.; Zhang, Z.; Liao, F.; Jiang, T.; Tu, Y. The Birth of Artemisinin. *Pharmacol. Ther.* **2020**, *216*, No. 107658.

(21) Guo, Z. Artemisinin Anti-Malarial Drugs in China. *Acta Pharm. Sin. B* **2016**, *6* (2), 115−124.

(22) Chen, K.; Tang, L.; Nong, X. Artesunate Targets Cellular Metabolism to Regulate the Th17/Treg Cell Balance. *Inflammation Res.* **2023**, *72* (5), 1037−1050.

(23) Zhang, S.; Li, J.; Nong, X.; Zhan, Y.; Xu, J.; Zhao, D.; Ma, C.; Wang, Y.; Li, Y.; Li, Z.; Li, J. Artesunate Combined With Metformin Ameliorate on Diabetes-Induced Xerostomia by Mitigating Superior Salivatory Nucleus and Salivary Glands Injury in Type 2 Diabetic Rats via the PI3K/AKT Pathway. *Front. Pharmacol.* **2021**, *12*, No. 774674, DOI: 10.3389/fphar.2021.774674.

(24) Chen, Y.; Li, W.; Nong, X.; Liang, C.; Li, J.; Lu, W.; Wang, B.; Yuan, Z.; Yang, S. Role of Artesunate on Cardiovascular Complications in Rats with Type 1 Diabetes Mellitus. *BMC Endocr. Disord.* **2021**, *21* (1), 19.

(25) Doshi, S. M.; Friedman, A. N. Diagnosis and Management of Type 2 Diabetic Kidney Disease. *Clin, J. Am. Soc. Nephrol.* **2017**, *12* (8), 1366−1373.

(26) Slyne, J.; Slattery, C.; McMorrow, T.; Ryan, M. P. New Developments Concerning the Proximal Tubule in Diabetic Nephropathy: *In Vitro* Models and Mechanisms. *Nephrol., Dial., Transplant.* **2015**, *30* (4), iv60−iv67.

(27) Chevalier, R. L. The Proximal Tubule Is the Primary Target of Injury and Progression of Kidney Disease: Role of the Glomerulotubular Junction. *Am. J. Physiol.: Renal Physiol.* **2016**, *311* (1), F145−F161.

(28) Vallon, V. The Proximal Tubule in the Pathophysiology of the Diabetic Kidney. *Am. J. Physiol.: Regul., Integr. Comp. Physiol.* **2011**, *300* (5), R1009−R1022.

(29) Liu, J.; Yang, J.-R.; Chen, X.-M.; Cai, G.-Y.; Lin, L.-R.; He, Y.-N. Impact of ER Stress-Regulated ATF4/P16 Signaling on the Premature Senescence of Renal Tubular Epithelial Cells in Diabetic Nephropathy. *Am. J. Physiol.: Cell Physiol.* **2015**, *308* (8), C621−C630.

(30) Zhang, X.; Chen, X.; Wu, D.; Liu, W.; Wang, J.; Feng, Z.; Cai, G.; Fu, B.; Hong, Q.; Du, J. Downregulation of Connexin 43 Expression by High Glucose Induces Senescence in Glomerular Mesangial Cells. *J. Am. Soc. Nephrol.* **2006**, *17* (6), 1532−1542.

(31) Sampson, M. J.; Hughes, D. A. Chromosomal Telomere Attrition as a Mechanism for the Increased Risk of Epithelial Cancers and Senescent Phenotypes in Type 2 Diabetes. *Diabetologia* **2006**, *49* (8), 1726−1731.

(32) Fyhrquist, F.; Tiitu, A.; Saijonmaa, O.; Forsblom, C.; Groop, P.-H. Telomere Length and Progression of Diabetic Nephropathy in Patients with Type 1 Diabetes. *J. Intern. Med.* **2010**, *267* (3), 278−286.

(33) Martindale, J. L.; Holbrook, N. J. Cellular Response to Oxidative Stress: Signaling for Suicide and Survival*. *J. Cell. Physiol.* **2002**, *192* (1), 1−15.

(34) Tesch, G. H.; Ma, F. Y.; Han, Y.; Liles, J. T.; Breckenridge, D. G.; Nikolic-Paterson, D. J. ASK1 Inhibitor Halts Progression of Diabetic Nephropathy in *Nos3* -Deficient Mice. *Diabetes* **2015**, *64* (11), 3903−3913.

https://doi.org/10.1021/acsomega.4c00020
ACS Omega 2024, 9, 16358−16373

(35) Stoyanovsky, D. A.; Tyurina, Y. Y.; Shrivastava, I.; Bahar, I.; Tyurin, V. A.; Protchenko, O.; Jadhav, S.; Bolevich, S. B.; Kozlov, A. V.; Vladimirov, Y. A.; Shvedova, A. A.; Philpott, C. C.; Bayir, H.; Kagan, V. E. Iron Catalysis of Lipid Peroxidation in Ferroptosis: Regulated Enzymatic or Random Free Radical Reaction? *Free Radical Biol. Med.* **2019**, *133*, 153−161.
(36) Ursini, F.; Maiorino, M. Lipid Peroxidation and Ferroptosis: The Role of GSH and GPx4. *Free Radical Biol. Med.* **2020**, *152*, 175−185.
(37) Kim, S.; Kang, S.-W.; Joo, J.; Han, S. H.; Shin, H.; Nam, B. Y.; Park, J.; Yoo, T.-H.; Kim, G.; Lee, P.; Park, J. T. Characterization of Ferroptosis in Kidney Tubular Cell Death under Diabetic Conditions. *Cell Death Dis.* **2021**, *12* (2), 160.
(38) Sanz, A. B.; Sanchez-Niño, M. D.; Ramos, A. M.; Ortiz, A. Regulated Cell Death Pathways in Kidney Disease. *Nat. Rev. Nephrol.* **2023**, *19* (5), 281−299.
(39) Fang, Y.; Tian, S.; Pan, Y.; Li, W.; Wang, Q.; Tang, Y.; Yu, T.; Wu, X.; Shi, Y.; Ma, P.; Shu, Y. Pyroptosis: A New Frontier in Cancer. *Biomed. Pharmacother.* **2020**, *121*, No. 109595.
(40) Wang, J.; Wen, Y.; Lv, L.; Liu, H.; Tang, R.; Ma, K.; Liu, B. Involvement of Endoplasmic Reticulum Stress in Angiotensin II-Induced NLRP3 Inflammasome Activation in Human Renal Proximal Tubular Cells in Vitro. *Acta Pharmacol. Sin.* **2015**, *36* (7), 821−830.
(41) Bauernfeind, F.; Bartok, E.; Rieger, A.; Franchi, L.; Núñez, G.; Hornung, V. Cutting Edge: Reactive Oxygen Species Inhibitors Block Priming, but Not Activation, of the NLRP3 Inflammasome. *J. Immunol.* **2011**, *187* (2), 613−617.
(42) Levine, B. Autophagy in Cell Death: An Innocent Convict? *J. Clin. Invest.* **2005**, *115* (10), 2679−2688.
(43) Mizushima, N.; Yoshimori, T.; Levine, B. Methods in Mammalian Autophagy Research. *Cell* **2010**, *140* (3), 313−326.
(44) Kajiwara, M.; Masuda, S. Role of MTOR Inhibitors in Kidney Disease. *Int. J. Mol. Sci.* **2016**, *17* (6), 975.
(45) Yang, C.; Chen, X.-C.; Li, Z.-H.; Wu, H.-L.; Jing, K.-P.; Huang, X.-R.; Ye, L.; Wei, B.; Lan, H.-Y.; Liu, H.-F. SMAD3 Promotes Autophagy Dysregulation by Triggering Lysosome Depletion in Tubular Epithelial Cells in Diabetic Nephropathy. *Autophagy* **2021**, *17* (9), 2325−2344.
(46) Xu, Y.; Wan, W. Acetylation in the Regulation of Autophagy. *Autophagy* **2023**, *19* (2), 379−387.
(47) Hardie, D. G.; Ross, F. A.; Hawley, S. A. AMPK: A Nutrient and Energy Sensor That Maintains Energy Homeostasis. *Nat. Rev. Mol. Cell Biol.* **2012**, *13* (4), 251−262.
(48) Han, Y.-c.; Tang, S.; Liu, Y.; Li, A.; Zhan, M.; Yang, M.; Song, N.; Zhang, W.; Wu, X.; Peng, C.; Zhang, H.; Yang, S. AMPK Agonist Alleviate Renal Tubulointerstitial Fibrosis via Activating Mitophagy in High Fat and Streptozotocin Induced Diabetic Mice. *Cell Death Dis.* **2021**, *12* (10), 925.
(49) Tan, E.; Gao, Z.; Wang, Q.; Han, B.; Shi, H.; Wang, L.; Zhu, G.; Hou, Y. Berberine Ameliorates Renal Interstitial Inflammation and Fibrosis in Mice with Unilateral Ureteral Obstruction. *Basic Clin. Pharmacol. Toxicol.* **2023**, *133*, 757.
(50) Jin, D.; Zhao, Y.; Sun, Y.; Xue, J.; Li, X.; Wang, X. Jiedu Tongluo Baoshen Formula Enhances Renal Tubular Epithelial Cell Autophagy to Prevent Renal Fibrosis by Activating SIRT1/LKB1/AMPK Pathway. *Biomed. Pharmacother.* **2023**, *160*, No. 114340.
(51) Miguel, V.; Tituaña, J.; Herrero, J. I.; Herrero, L.; Serra, D.; Cuevas, P.; Barbas, C.; Puyol, D. R.; Márquez-Expósito, L.; Ruiz-Ortega, M.; Castillo, C.; Sheng, X.; Susztak, K.; Ruiz-Canela, M.; Salas-Salvadó, J.; González, M. A. M.; Ortega, S.; Ramos, R.; Lamas, S. Renal Tubule Cpt1a Overexpression Protects from Kidney Fibrosis by Restoring Mitochondrial Homeostasis. *J. Clin. Invest.* **2021**, *131* (5), No. e140695, DOI: 10.1172/JCI140695.
(52) Tang, P. M.-K.; Nikolic-Paterson, D. J.; Lan, H.-Y. Macrophages: Versatile Players in Renal Inflammation and Fibrosis. *Nat. Rev. Nephrol.* **2019**, *15* (3), 144−158.
(53) Wu, S.-H.; Lu, C.; Dong, L.; Zhou, G.-P.; He, Z.-G.; Chen, Z.-Q. Lipoxin A4 Inhibits TNF-α-Induced Production of Interleukins and Proliferation of Rat Mesangial Cells. *Kidney Int.* **2005**, *68* (1), 35−46.
(54) White, J.; Suklabaidya, S.; Vo, M. T.; Choi, Y. B.; Harhaj, E. W. Multifaceted Roles of TAX1BP1 in Autophagy. *Autophagy* **2023**, *19* (1), 44−53.
(55) Du, L.; Chen, Y.; Shi, J.; Yu, X.; Zhou, J.; Wang, X.; Xu, L.; Liu, J.; Gao, J.; Gu, X.; Wang, T.; Yin, Z.; Li, C.; Yan, M.; Wang, J.; Yin, X.; Lu, Q. Inhibition of S100A8/A9 Ameliorates Renal Interstitial Fibrosis in Diabetic Nephropathy. *Metabolism* **2023**, *144*, No. 155376.
(56) O'Sullivan, E. D.; Mylonas, K. J.; Xin, C.; Baird, D. P.; Carvalho, C.; Docherty, M.-H.; Campbell, R.; Matchett, K. P.; Waddell, S. H.; Walker, A. D.; Gallagher, K. M.; Jia, S.; Leung, S.; Laird, A.; Wilflingseder, J.; Willi, M.; Reck, M.; Finnie, S.; Pisco, A.; Gordon-Keylock, S.; Medvinsky, A.; Boulter, L.; Henderson, N. C.; Kirschner, K.; Chandra, T.; Conway, B. R.; Hughes, J.; Denby, L.; Bonventre, J. V.; Ferenbach, D. A. Indian Hedgehog Release from TNF-Activated Renal Epithelia Drives Local and Remote Organ Fibrosis. *Sci. Transl. Med.* **2023**, *15* (698), No. eabn0736, DOI: 10.1126/scitranslmed.abn0736.
(57) Cui, X.; Li, Y.; Yuan, S.; Huang, Y.; Chen, X.; Han, Y.; Liu, Z.; Li, Z.; Xiao, Y.; Wang, Y.; Sun, L.; Liu, H.; Zhu, X. Alpha-kinase1 Promotes Tubular Injury and Interstitial Inflammation in Diabetic Nephropathy by Canonical Pyroptosis Pathway. *Biol. Res.* **2023**, *56* (1), 5.
(58) Li, F.; Chen, Y.; Li, Y.; Huang, M.; Zhao, W. Geniposide Alleviates Diabetic Nephropathy of Mice through AMPK/SIRT1/NF-KB Pathway. *Eur. J. Pharmacol.* **2020**, *886*, No. 173449.
(59) Popov, S. V.; Mukhomedzyanov, A. V.; Voronkov, N. S.; Derkachev, I. A.; Boshchenko, A. A.; Fu, F.; Sufianova, G. Z.; Khlestkina, M. S.; Maslov, L. N. Regulation of Autophagy of the Heart in Ischemia and Reperfusion. *Apoptosis* **2023**, *28* (1−2), 55−80.
(60) Lehto, M.; Groop, P.-H. The Gut-Kidney Axis: Putative Interconnections Between Gastrointestinal and Renal Disorders. *Front. Endocrinol.* **2018**, *9*, No. 389053, DOI: 10.3389/fendo.2018.00553.
(61) Shen, Z.; Cui, T.; Liu, Y.; Wu, S.; Han, C.; Li, J. Astragalus Membranaceus and Salvia Miltiorrhiza Ameliorate Diabetic Kidney Disease via the "Gut-Kidney Axis". *Phytomedicine* **2023**, *121*, No. 155129.
(62) Lu, C.-c.; Hu, Z.; Wang, R.; Hong, Z.; Lu, J.; Chen, P.; Zhang, J.; Li, X.; Yuan, B.; Huang, S.; Ruan, X.; Liu, B.; Ma, K. Gut Microbiota Dysbiosis-Induced Activation of the Intrarenal Renin−Angiotensin System Is Involved in Kidney Injuries in Rat Diabetic Nephropathy. *Acta Pharmacol. Sin.* **2020**, *41* (8), 1111−1118.
(63) Peti-Peterdi, J. High Glucose and Renin Release: The Role of Succinate and GPR91. *Kidney Int.* **2010**, *78* (12), 1214−1217.
(64) Gasaly, N.; de Vos, P.; Hermoso, M. A. Impact of Bacterial Metabolites on Gut Barrier Function and Host Immunity: A Focus on Bacterial Metabolism and Its Relevance for Intestinal Inflammation. *Front. Immunol.* **2021**, *12*, No. 658354, DOI: 10.3389/fimmu.2021.658354.
(65) Cai, K.; Ma, Y.; Cai, F.; Huang, X.; Xiao, L.; Zhong, C.; Ren, P.; Luo, Q.; Chen, J.; Han, F. Changes of Gut Microbiota in Diabetic Nephropathy and Its Effect on the Progression of Kidney Injury. *Endocrine* **2022**, *76* (2), 294−303.
(66) Ni, Y.; Zheng, L.; Nan, S.; Ke, L.; Fu, Z.; Jin, J. Enterorenal Crosstalks in Diabetic Nephropathy and Novel Therapeutics Targeting the Gut Microbiota. *Acta Biochim. Biophys. Sin.* **2022**, *54* (10), 1406−1420.
(67) Herman-Edelstein, M.; Weinstein, T.; Levi, M. Bile Acid Receptors and the Kidney. *Curr. Opin. Nephrol. Hypertens.* **2018**, *27* (1), 56−62.
(68) Wang, P.; Wang, T.; Zheng, X.; Cui, W.; Shang, J.; Zhao, Z. Gut Microbiota, Key to Unlocking the Door of Diabetic Kidney Disease. *Nephrology* **2021**, *26* (8), 641−649.
(69) Mosterd, C. M.; Kanbay, M.; van den Born, B. J. H.; van Raalte, D. H.; Rampanelli, E. Intestinal Microbiota and Diabetic Kidney Diseases: The Role of Microbiota and Derived Metabolites

Inmodulation of Renal Inflammation and Disease Progression. *Best Pract. Res., Clin. Endocrinol. Metab.* **2021**, *35* (3), No. 101484.
(70) Fang, Q.; Zheng, B.; Liu, N.; Liu, J.; Liu, W.; Huang, X.; Zeng, X.; Chen, L.; Li, Z.; Ouyang, D. Trimethylamine N-Oxide Exacerbates Renal Inflammation and Fibrosis in Rats With Diabetic Kidney Disease. *Front. Physiol.* **2021**, *12*, No. 682482, DOI: 10.3389/fphys.2021.682482.
(71) Snelson, M.; de Pasquale, C.; Ekinci, E. I.; Coughlan, M. T. Gut Microbiome, Prebiotics, Intestinal Permeability and Diabetes Complications. *Best Pract. Res., Clin. Endocrinol. Metab.* **2021**, *35* (3), No. 101507.
(72) Sun, C.-Y.; Chang, S.-C.; Wu, M.-S. Uremic Toxins Induce Kidney Fibrosis by Activating Intrarenal Renin−Angiotensin−Aldosterone System Associated Epithelial-to-Mesenchymal Transition. *PLoS One* **2012**, *7* (3), No. e34026.
(73) Lu, C. C.; Ma, K. L.; Ruan, X. Z.; Liu, B. C. Intestinal Dysbiosis Activates Renal Renin-Angiotensin System Contributing to Incipient Diabetic Nephropathy. *Int. J. Med. Sci.* **2018**, *15* (8), 816−822.
(74) Bao, J.; Li, L.; Zhang, Y.; Wang, M.; Chen, F.; Ge, S.; Chen, B.; Yan, F. Periodontitis May Induce Gut Microbiota Dysbiosis via Salivary Microbiota. *Int. J. Oral Sci.* **2022**, *14* (1), 32.

https://doi.org/10.1021/acsomega.4c00020
ACS Omega 2024, 9, 16358−16373